# RESONANCE TUBES

by

PHILIP A. THOMPSON

S.B., Rensselaer Polytechnic Institute
(1957)

S.M., Rensselaer Polytechnic Institute
(1958)

SUBMITTED IN PARTIAL FULFILLMENT

OF THE REQUIREMENTS FOR THE

DEGREE OF DOCTOR OF

SCIENCE

at the

MASSACHUSETTS INSTITUTE OF TECHNOLOGY

December, 1960

Signature of Author.....
Department of Mechanical Engineering
December 14, 1960

Certified by.....
Thesis Supervisor

Accepted by.....
Chariman, Departmental Committee
on Graduate Students

# RESONANCE TUBES

by

Philip A. Thompson

Submitted to the Department of Mechanical Engineering on December 14, 1960 in partial fulfillment of the requirements for the degree of Doctor of Science.

## ABSTRACT

A simple resonance tube consists of a cylinder, one end of which is closed, the other end open. A jet of gas directed axially against the open end may excite the gases within the tube to violent oscillation. Straight or periodic supersonic jets are most effective for this excitation. Timed shadowgraphs of the external flow have been made; transducer pressure records at the open and closed ends of the tube have been obtained. External flow is temporarily steady during the tube inflow and outflow phases. Internal flow includes transiting shock waves of moderate strength with consequent irreversible heating of the tube. By the application of flow boundary conditions, wave diagrams for the internal flow have been constructed. Pressure histories obtained from the wave diagrams agree well with the experimental pressure records. Heating effects have been estimated from the computed entropy production.

Thesis Supervisor: Ascher H. Shapiro

Title: Professor of Mechanical Engineering

## ACKNOWLEDGEMENTS

The author is indebted to Professor Ascher H. Shapiro for the patient supervision of this thesis. Gratitude is expressed to Professor Harold E. Edgerton, who has loaned essential equipment and given advice, to Professors James A. Fay and Gerald B. Whitham for serving on the thesis committee, and to the National Science Foundation, which has supported the author's graduate study.

## TABLE OF CONTENTS

## LIST OF FIGURES

# I THE PROBLEM

A simple resonance tube consists of a straight cylinder, one end of which is closed, the other end open. A jet of gas, directed axially against the open end, may excite the gases within the tube to strong longitudinal oscillation. Supersonic jets, either straight or periodic, are effective.

Figure 1 shows a typical arrangement.

Resonance tubes are interesting because the gas oscillations may be violent. When properly excited, the internal flow will include shock waves of moderate strength, transiting the tube a few hundred times per second. These shock waves can effect a strong heating of the gas trapped within the tube.

This thesis sets out to describe the flow in resonance tubes, the external flows, and the heating effects. The problem has been studied by high speed motion pictures, shadowgraphs, and wave diagram analysis.

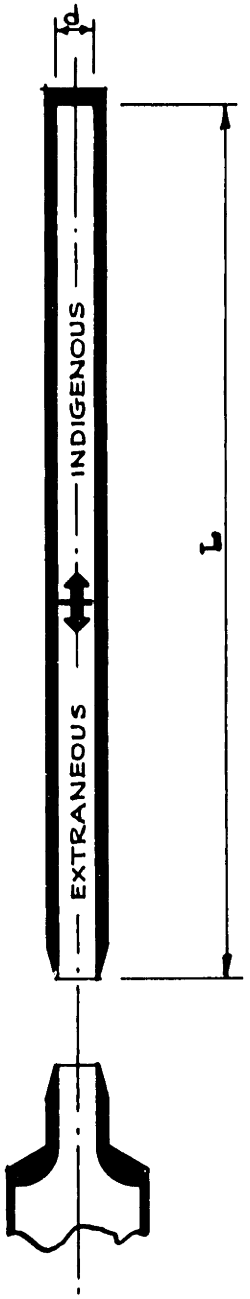


FIG. 1: A REPRESENTATIVE RESONANCE TUBE

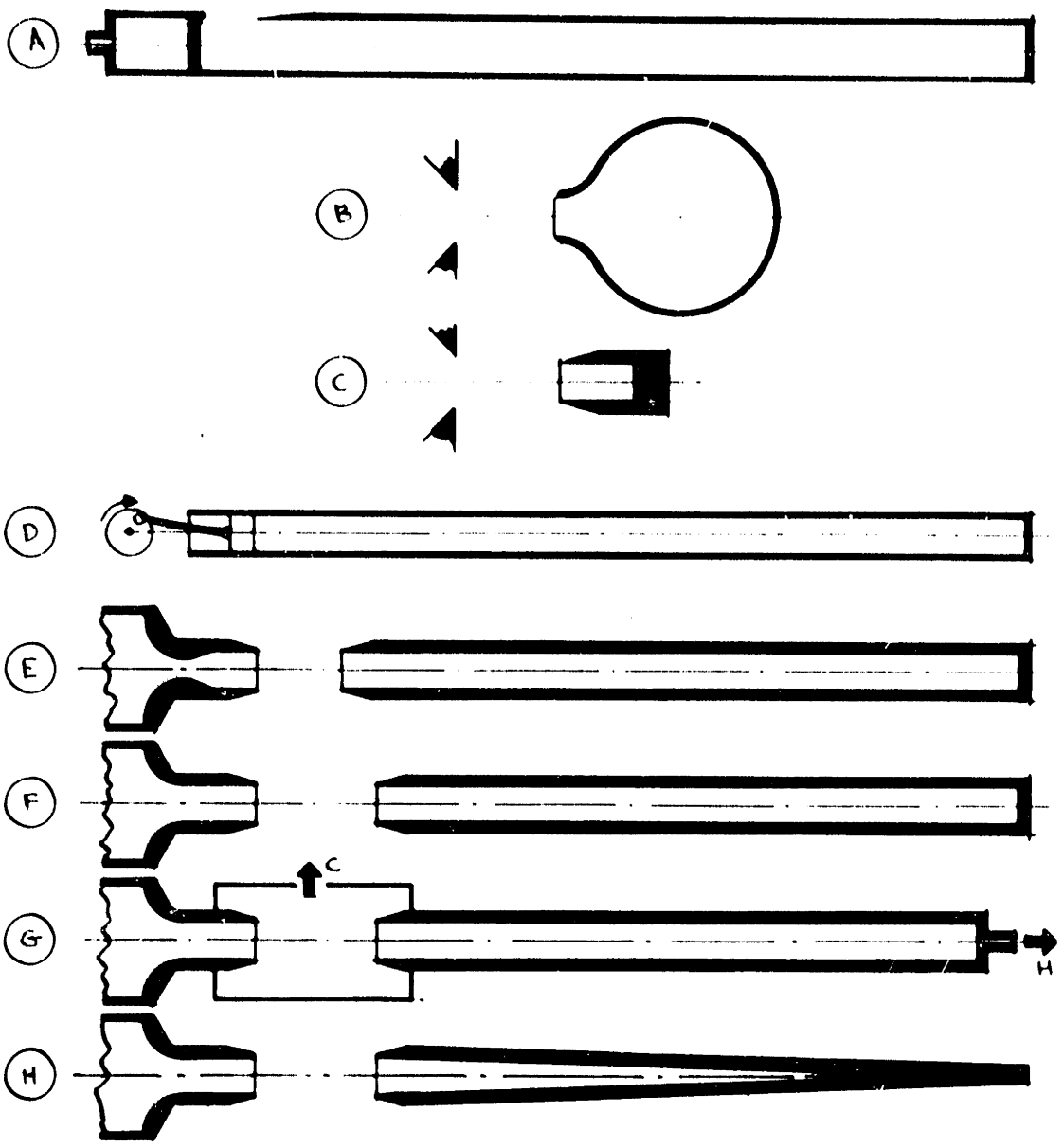


FIG. 2: DEMONSTRATED RESONANCE DEVICES

A. ORGAN PIPE
B. HARTMANN'S PULSATOR
C. HARTMANN'S OSCILLATOR
D. PISTON-DRIVEN TUBE
E. SIMPLE TUBE - SUPERSONIC JET
F. SIMPLE TUBE - PERIODIC JET
G. SPRENGER'S SEPARATOR
H. TAPERED TUBE (ANALOGUE)

## II HISTORY

The device now called a resonance tube was first described by Hartmann[2] in 1919, and designated by him the "air-jet oscillator". Because he was interested in the ultrasonic waves radiated from the tube mouth, Hartmann used a very short tube, about two diameters in length. It was excited by the periodic jet from an underexpanded sonic nozzle. Hartmann found that the oscillator would resonate when the mouth of the tube was placed in one of the converging zones of the jet - the interval of instability. He also demonstrated a device like a Helmholtz Resonator, "the air-jet pulsator", similarly excited but having a much longer period, in the order of a few minutes.

Lettau[3] and others have demonstrated resonant effects in a very long closed tube, one end of which is formed by a movable piston. At critical piston frequencies, shock waves have been observed. The problem has been analyzed by Frederiksen[4] and Betchov[5]. Since the amplitude within piston driven tubes has been very small, however, they are not comparable to

resonance tubes.*

Sprenger[6] has published extensive experimental results for a resonance tube 0.3 cm. in diameter and 10.2 cm. in length. He found resonant excitation possible by either a periodic or a straight supersonic jet. With excitation by a periodic jet at a reservoir pressure of five atmospheres, wall temperature at the closed end of the tube reached 500 °C. After the accidental introduction of fine particles into the tube (melted solder), a wall temperature of over 1000 °C was obtained.

Sprenger also applied the resonance tube as a temperature separator, by permitting hot gas to escape from an orifice in the (normally) closed end. The effect was very close to that achieved by the Ranque-Hilsch vortex tube.

Some of Sprenger's results with periodic jets have been extended by Howick and Hughes[7], and by Cassidy, Thompson, and Slawsky[8]. These two groups have also obtained transducer pressure records which clearly indicate the presence of shock waves. Cassidy, et al.

*The tube length in Lettau's experiments was 353 times the piston amplitude. In the case of a resonance tube, the amplitude is about three-fourths of the tube length.

obtained Schlieren photographs of the internal flow.

Sibulkin and Vrebalovich[9] obtained strong oscillations in a tube mounted in a 12-inch wind tunnel, Mach Number 2.8.

Lloyd[10] has made smear pictures of the flow within a square resonance tube, giving a partial wave diagram.* Fam[11] has obtained shadowgraphs of the internal flow.

It was recognized by Sprenger[13] and others that the accidental inclusion of resonance-tube like configurations in pneumatic systems constituted an accident hazard. It has been reported that machine gun barrels in transonic aircraft have become red hot, probably through resonance tube effects.

## The organ pipe

The closed organ pipe, dating from the third century B. C. or earlier, is obviously somewhat similar to a resonance tube. The oscillations in an organ

*The workers at the Bureau of Standards (8,10) used periodic jets from nozzles of square cross section. It is remarkable that the perturbation solution for a jet from a square orifice is precisely periodic. (reference 21, p46).

are linear, however, while those in a resonance tube are interesting just because of their strong non-linearity. Further, the means of excitation are quite different.

Hartenbaum's experiments

A detailed report on the hydraulic analogue to resonance tubes has been made by Hartenbaum[12]. Various aspects of the gas flow problem form the substance of this report and will be discussed later. It may be interesting, however, to mention some of Hartenbaum's results with the hydraulic analogue. He worked principally with periodic jets, discharging into a half-inch depth water atmosphere.

It was striking that the hydraulic tube did not resonate when the test flume was level, but worked nicely with a downstream tilt of merely .07 degrees! This indicates the great influence of the flume skin friction, which thus spoils the two-dimensionality of the model.

The train of shocklets seen in the analogue shadowgraphs is similar to trains photographed by Cassidy, et al. in their resonance tube. However, there is no

connection: the train seen in the analogue is characteristic of hydraulic bores; the train seen in Cassidy's photographs seem to result from the refocusing of the periodic jet near the mouth of the tube.

Although the analogue was effective in the case of periodic jets, operation for correctly expanded supercritical jets was discouragingly disparate from the gas flow. The hydraulic oscillation in this case was like that of an organ pipe.

In experiments with a tapered tube, Hartenbaum found very great head rises at the closed end.

## III GENERAL FEATURES OF THE FLOW

At the beginning of this study, almost nothing was known about the mode of excitation. Data of earlier investigators pertained to the internal pressure history and the tube heating. However, in the absence of knowledge about the interaction between jet and tube flows, no comprehensive description of the internal flow is possible. If the interaction be known in detail, construction of the internal flow follows from well known procedures using the method of characteristics.

Thus, an obvious first step was to photograph the external flow.

### The experimental arrangement

High speed motion picture shadowgraphs were made, using a small high speed stroboscopic lamp flashing at a rate of 5000/sec and duration of one microsecond. Since the flash duration was so brief, no camera shutter was required. The 16 mm Fastax camera employed was thus run with the prism (which normally functions as a shutter) removed. A regular flashing rate was

achieved by using signals from an oscillator. In this way, the frames obtained were separated by fixed intervals of time and served to 'clock' the behavior of the jet.

The image (that is, the shadow pattern) photographed by the high speed camera appeared on a ground glass mounted opposite the light source, with the gas flow intervening.

Because the definition on the high speed films was poor, conventional 4 x 5 inch shadowgraphs were also made. Since the movie frames showed a precisely periodic flow, it was possible to accurately fix the sequence and time for each random shadowgraph.

The resonance tube was made of stainless steel, one-half inch in inside diameter, and about twenty inches in length. The tube was mounted on a lathe cross slide, permitting the nozzle-tube spacing to be conveniently varied. Two different nozzles of one half inch diameter were employed; one supersonic, Mach Number 1.92, one simple converging.

Pressure records of the internal flow were obtained by a quartz crystal transducer mounted optionally at the closed or open end.

A detailed description of the apparatus appears

in Appendix B.

All of the experiments were made with air, which will be treated as a perfect gas.

## Note on terminology

Most experiments were performed with the aforementioned cylindrical tube. Such tubes will be designated "simple resonance tubes".

An underexpanded sonic jet (converging nozzle) and a correctly expanded supersonic jet (supersonic nozzle) were employed. The underexpanded jet is not truly periodic, since irreversible changes occur at the nodal shocks and viscous, turbulent, and conductive effects develop. For the sake of conciseness, however, such jets will be referred to simply as "periodic jets".

Correctly expanded supersonic jets will be designated "supersonic jets".

## General features

The two cases tested, "simple tube excited by a periodic jet", and "simple tube excited by a supersonic jet" are considered separately in following sections. The remarks made here will apply to <u>both</u> cases.

The flow photographs and pressure records were used to deduce some of the general properties of the flow described hereafter. These properties lead to a more detailed analysis for the simpler case, that of the tube excited by a supersonic jet.

To the experimenter, the first and unavoidable observation is that the operating tube produces a very intense noise, something like that from a factory whistle.* In addition to this, there are five salient points.

i) Resonance is very easy to obtain for a great variety of conditions: subsonic, periodic, and supersonic jets; various tube nozzle spacings; various tube lengths; various tube mouth shapes.

ii) Under favorable conditions the oscillations are very strong, the entire jet being "swallowed" by the tube for about one-third of the oscillation period.

iii) The inflow and the outflow phases are each temporarily steady. That is, they persist for substantial portions of one period without much change.

iv) The outflow impulse matches the jet impulse quite closely, so that the collision interface (separating gas from the jet and gas from the tube) is plane.

*Sprenger recorded a maximum sound intensity of 115 db. The intensity from the much larger tube used in the experiments discussed here was undoubtedly higher.

v) Irreversible internal flows (i.e. - transiting shock waves) produce a marked heating of the tube toward the closed end.

The period of oscillation, designated B, is about equal to the quarter wave acoustic period; that is, to the time required for four transits of the tube length by a sound wave at a speed corresponding to jet stagnation temperature. (For the tube used, the acoustic period is 6 ms.). One period can be divided into the following flow phases:

Temporarily steady inflow (about 37% B):

All of the jet mass flow passes into the tube. A shock stands near the mouth.

Transition from inflow to outflow (about 6% B):

This transition is announced very suddenly by the exit of a strong shock from the tube mouth. As the shock advances into the jet, the outflow is quickly established.

Temporarily steady outflow (about 33% B):

The outflow is about sonic at the tube mouth, but expands, with distance, to supersonic speed. The outflow and jet collide with a plane interface, each flow having passed through a decelerating shock.

Transition from outflow to inflow (about 24% B):

Compared to the previous transition, this is very slow. As the tube outflow weakens, the collision system recedes, finally passing into the tube mouth.

Shadowgraphs illustrating these phases are in figure 10.

The flow inside the tube may be roughly constructed as follows: As the outflow weakens, during transition to inflow, a shock moves into the tube while another shock stands at the mouth. The moving shock is reflected at the closed end and moves back toward the mouth. As it emerges from the tube, outflow is quickly established by the reflected rarefaction.

By using an over-simplified model, a striking matching between outflow strength and jet strength is obtained, in agreement with the observed plane collision interface. Beginning with the fluid about to enter the tube, the model gives the following processes:

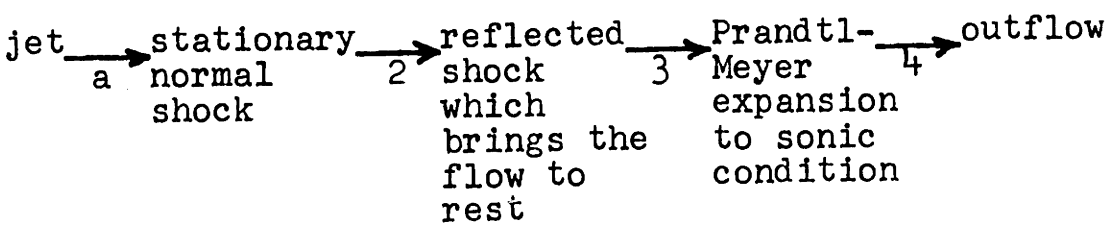


where a, 2, 3, and 4 refer to the fluid states. In Appendix H, it is shown that the impulse for state a (jet impulse) is very nearly equal to the impulse for state 4 (outflow impulse). The impulse ratio $J_4/J_a$

is plotted as a function of supersonic jet Mach Number in figure 21.

For periodic motions, the fluid always remaining within the tube is distinguished as "indigenous fluid". It is subjected to repeated shock waves and hence, continuous entropy creation. In a periodic flow, the reduction of entropy by heat transfer must exactly balance this entropy creation. However, this equilibrium condition is reached only after many initial cycles, during which the entropy (and hence the temperature) of the indigenous fluid is increasing. The tube may thus become very hot.*

The fluid which enters the tube during inflow and is expelled during outflow is here called "extraneous fluid". It is separated from indigenous fluid by a strong entropy discontinuity (hence a strong temperature discontinuity) and is subject to an entropy rise only during one cycle, after which it is expelled, to be replaced by new fluid from the jet.

*The indigenous fluid may be described in thermodynamic terms as a reversed perpetual motion machine of the second kind ($PMM_2$). That is, it forms a system operating in a cycle which receives work and rejects heat to a single reservoir.

It is convenient to think of the aforementioned interface as a massless piston, the motion of which follows that of the gas. At maximum compression, this 'piston' comes within $L/4$ of the closed end, where $L$ is the tube length.

## Stability and resonance zones

Prior studies have mostly employed periodic jets for excitation. Some elementary discussion of the source of instability in this case follows.

Shadowgraphs of periodic jets issuing from a sonic nozzle appear in figure 3. Such jets have been treated in numerous papers (14, 15, 16, 17, 18). The inviscid, shock-free flow can of course be solved by the method of characteristics.

Hartmann pointed out that in order to obtain oscillation, the resonance tube mouth must be placed in the converging region of one of the nearly periodic cells. This has been confirmed by subsequent investigators.

A simplified explanation for the initial instability of such flows is illustrated in figure 5. The undulatory curve represents the stagnation pressure

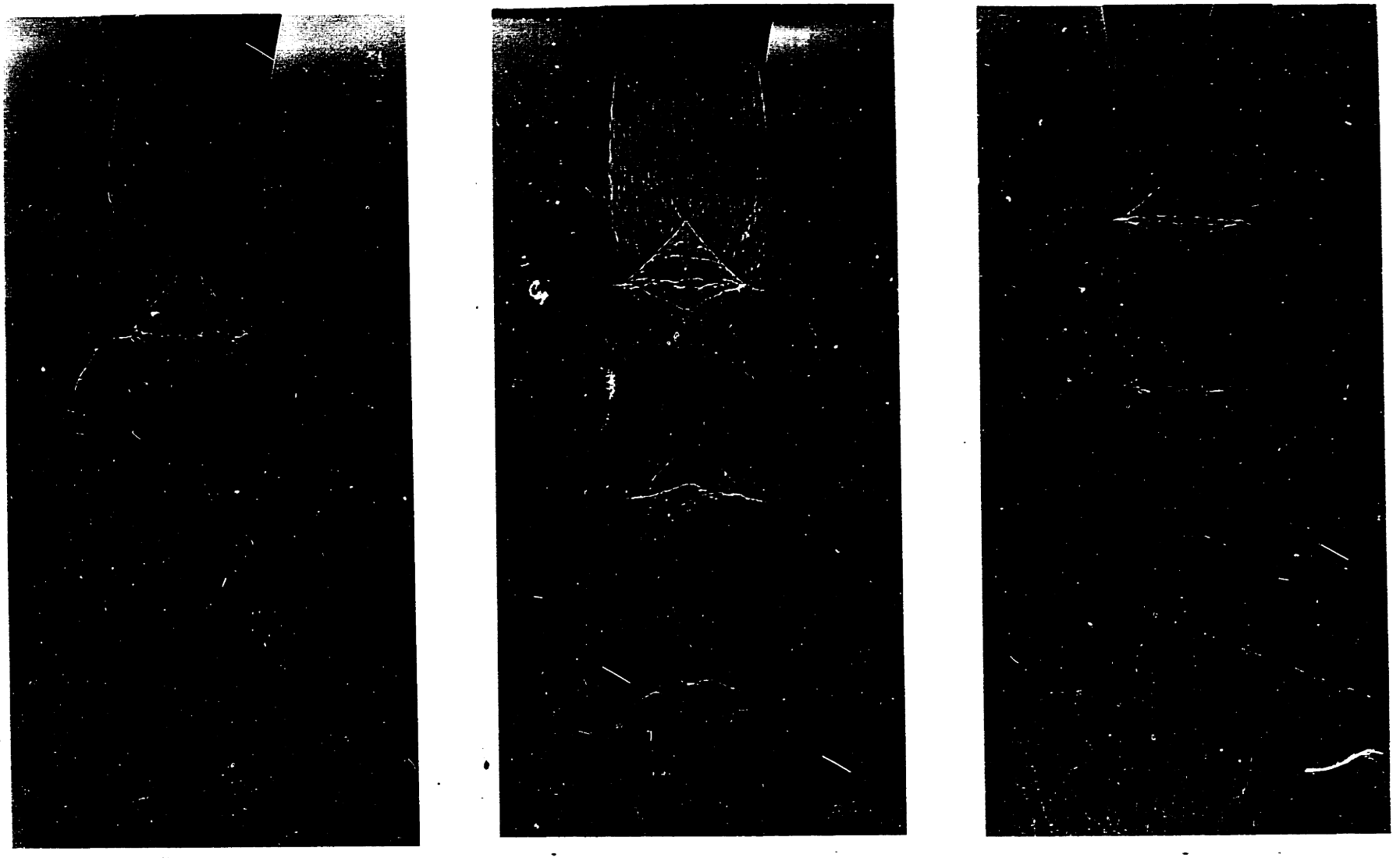

50 psig

40 psig

30 psig

Figure 3: Underexpanded Sonic Jet

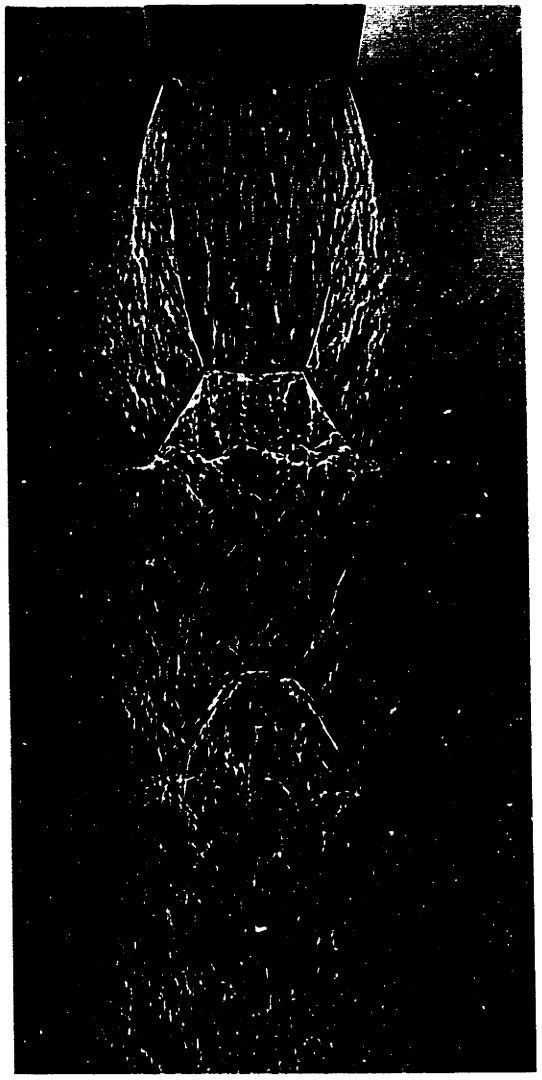

80 psig

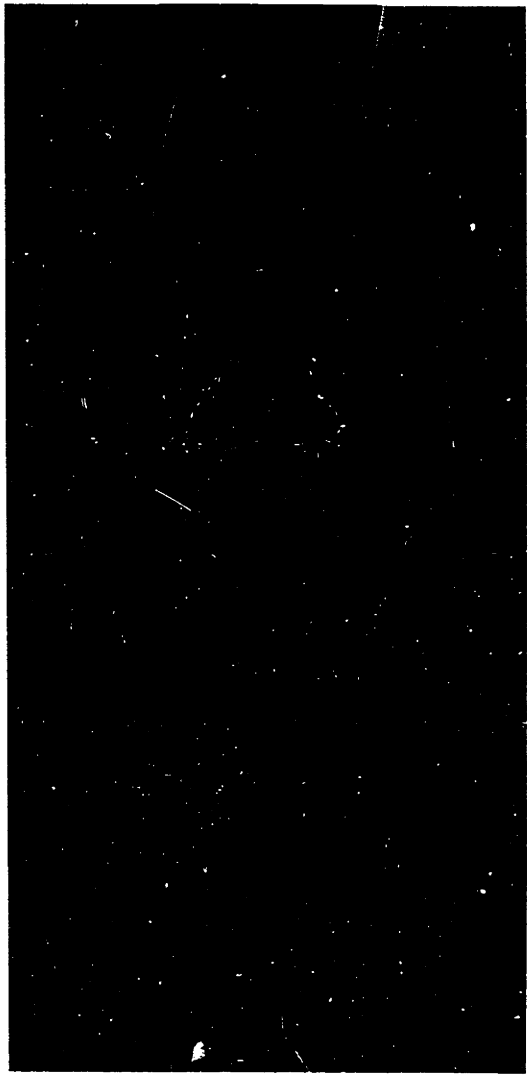

70 psig

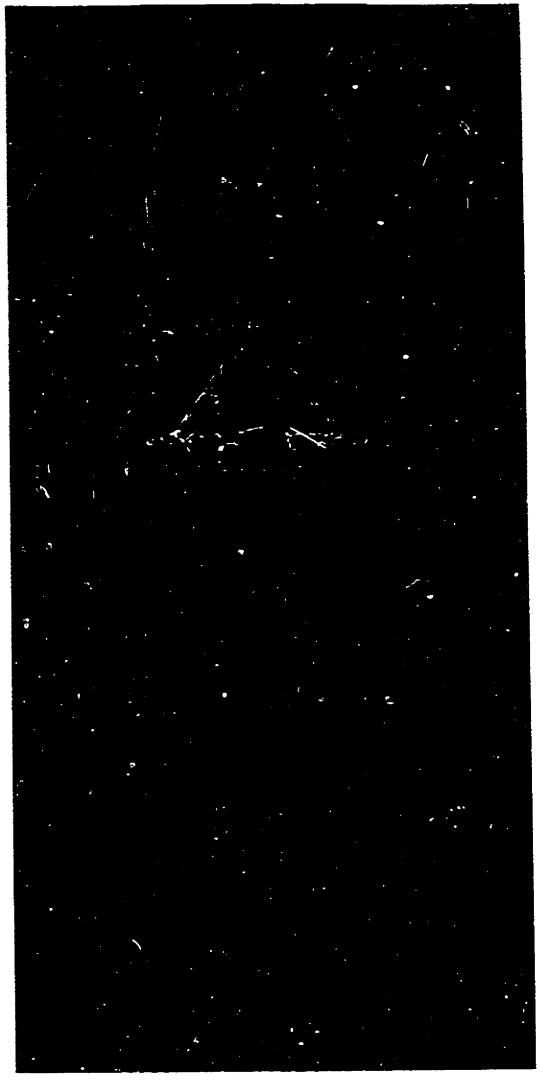

60 psig

Figure 3 (continued)

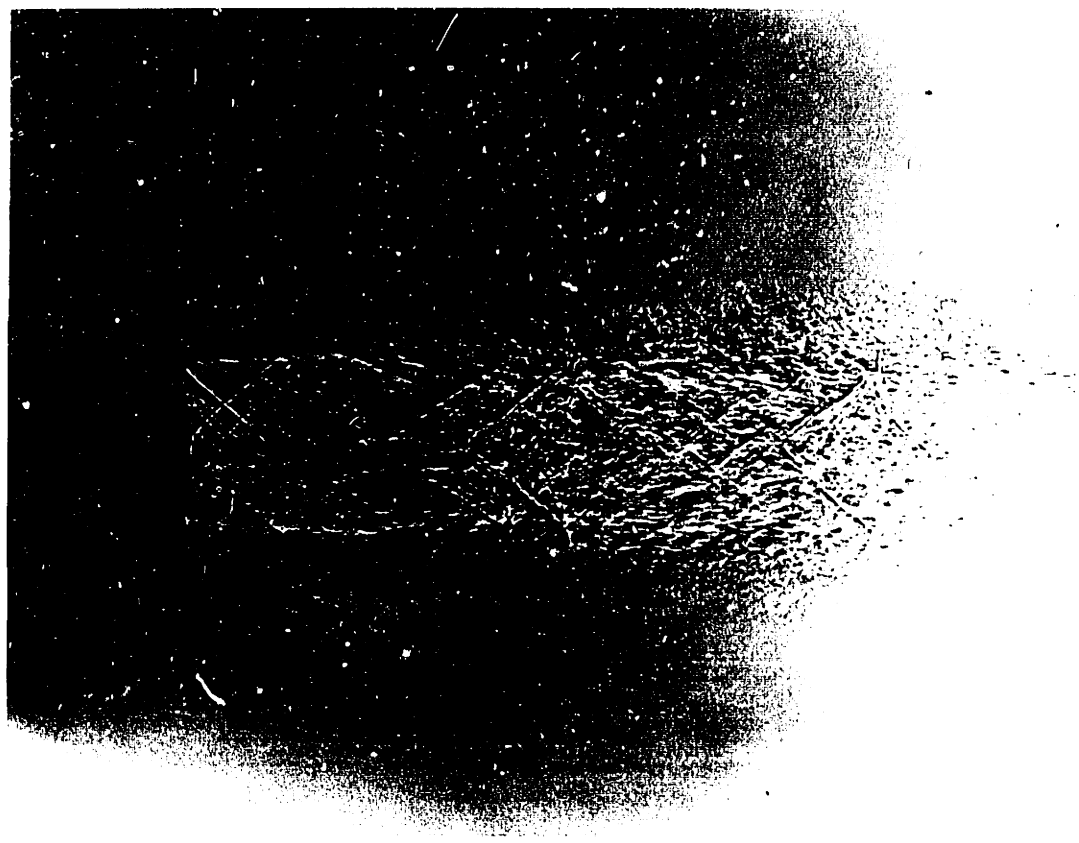

Figure 4: Supersonic Jet

Mach No. 1.92

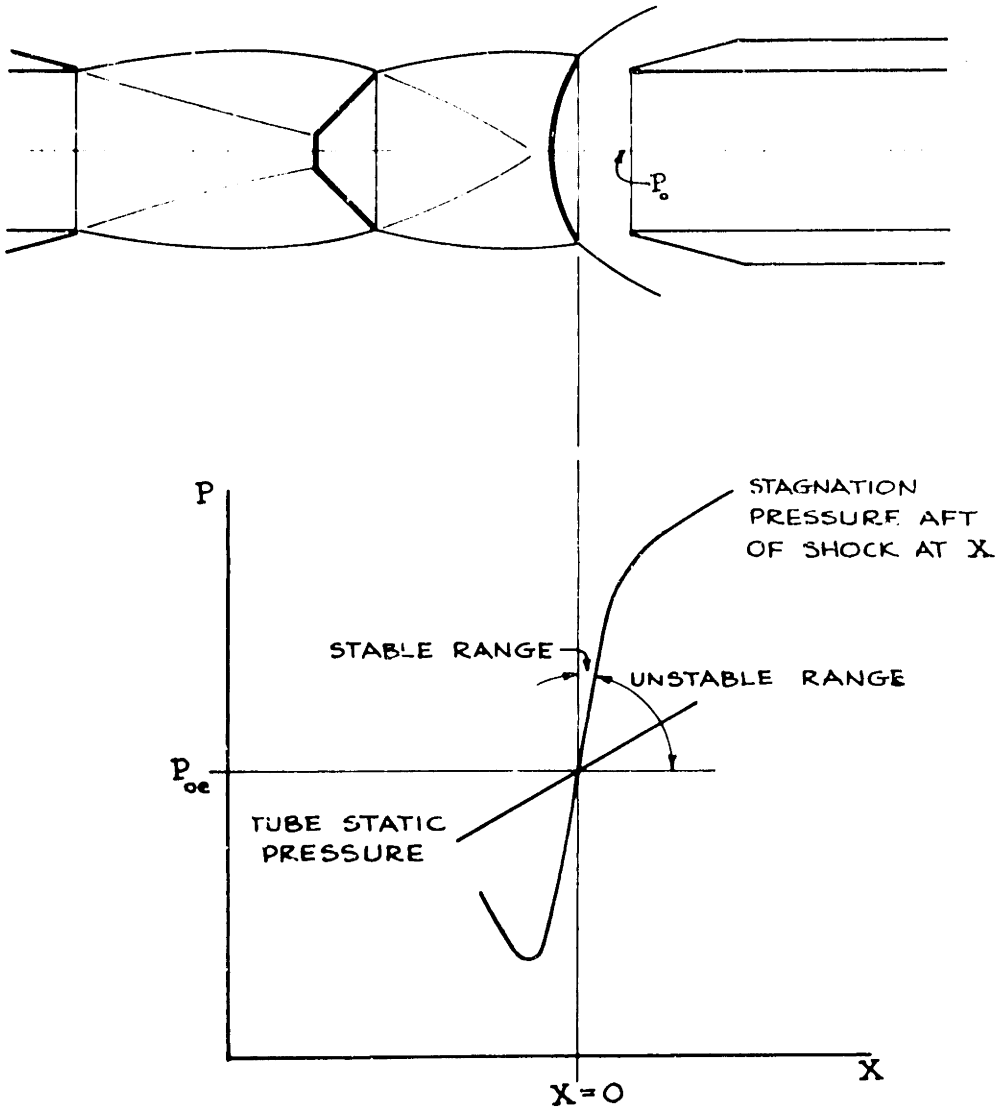


FIG. 5: STATIC INSTABILITY OF SHOCK IN A PERIODIC JET

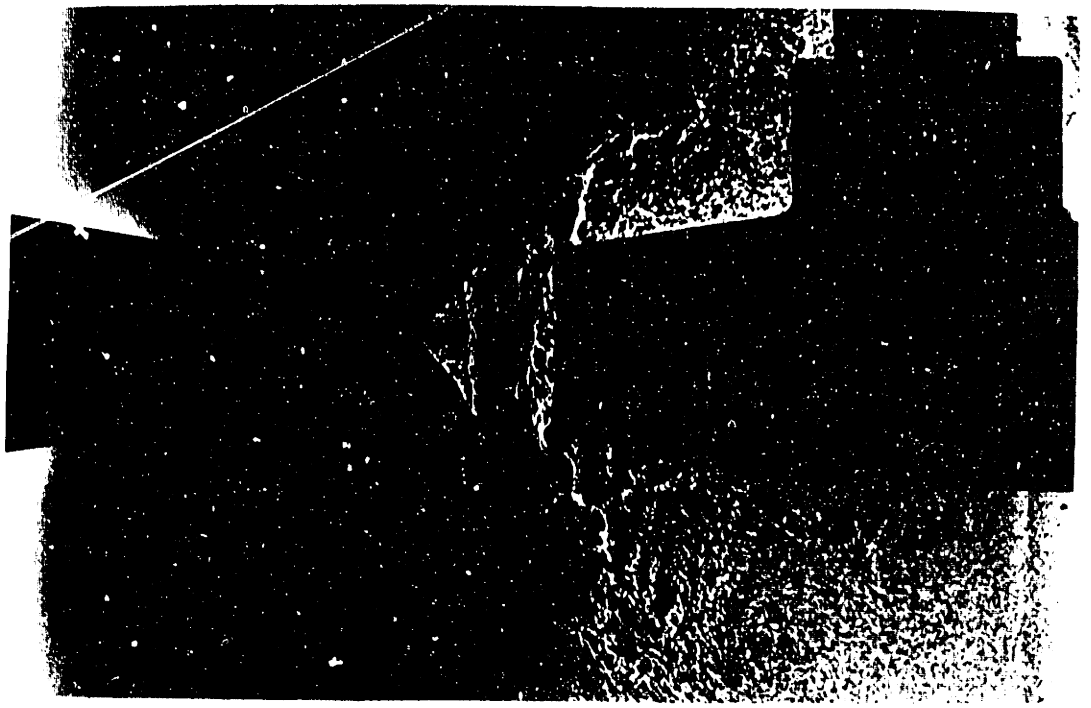

Fig. 6-1: Stable shock in supersonic jet, reservoir pressure 84 psig, separation 1.100 in.

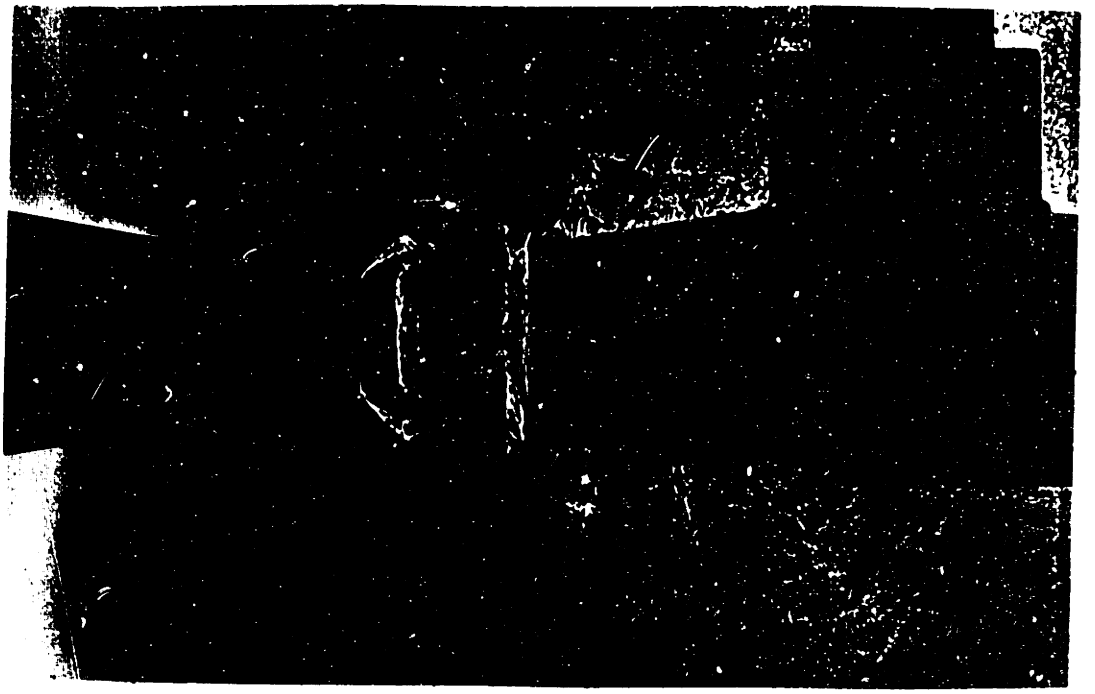

Fig. 6-2: Unstable shocks in periodic jet, reservoir pressure 60 psig, separation 1.00 in.

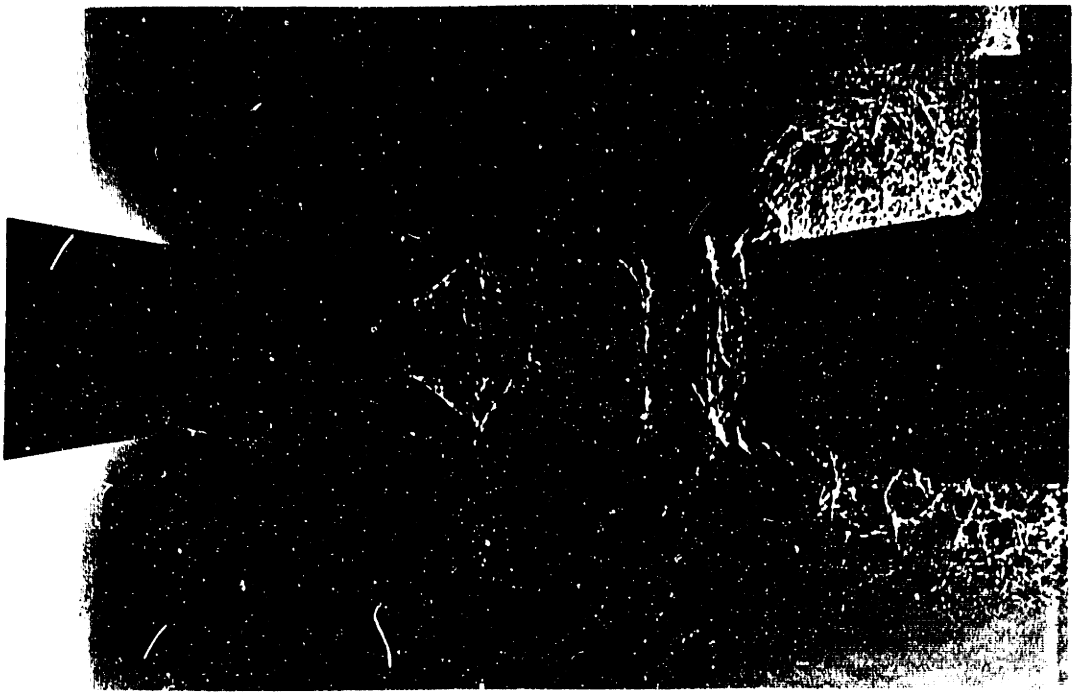

6-3: Unstable shocks in periodic jet, reservoir pressure 60 psig, separation 1.600 in.

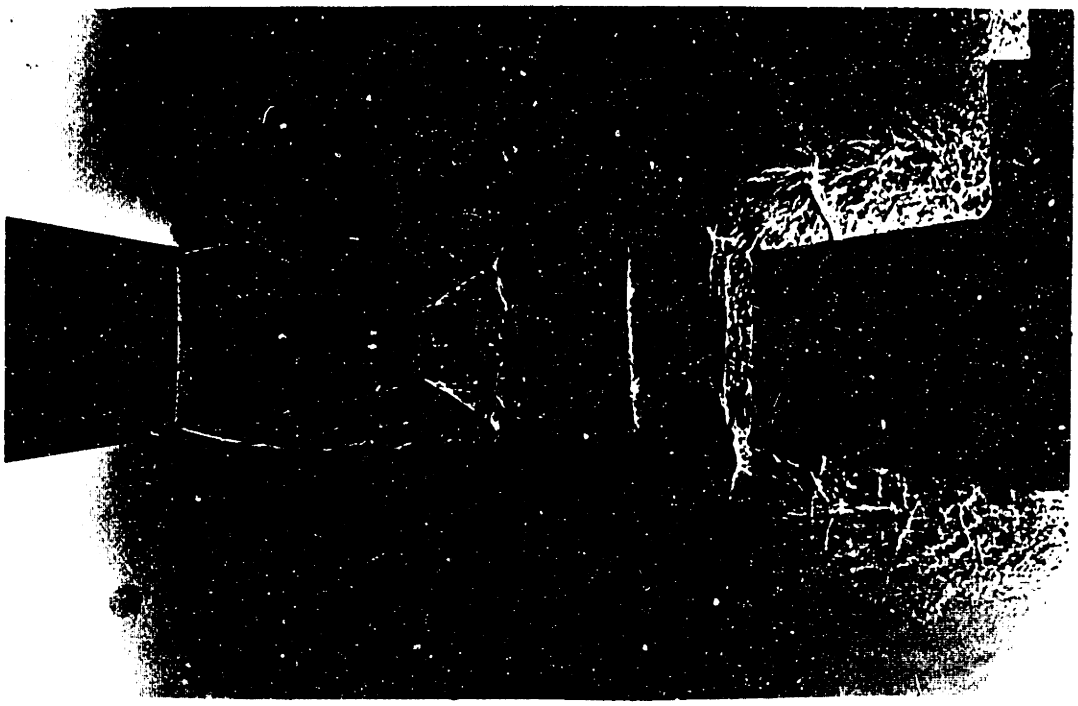

6-4: Unstable shocks in periodic jet, reservoir pressure 60 psig, separation 1.600 in.

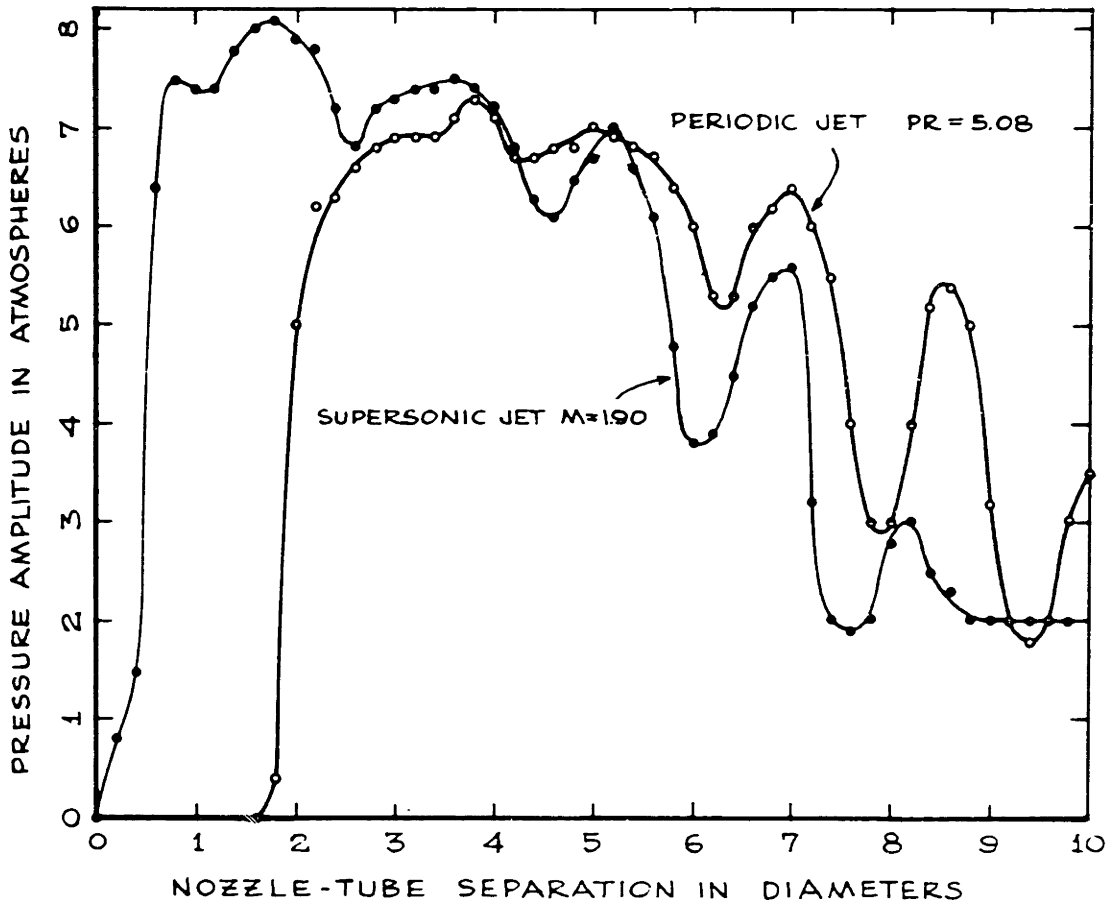


FIG. 7: PRESSURE AMPLITUDE vs. SEPARATION

aft of a shock occuring at X. The straight line represents the pressure-length relation for quasi-static compression of the fluid. A displacement of the shock from the equilibrium position results in a pressure difference tending to increase the displacement (i.e. - to compress the tube fluid), so long as the slope of the stagnation pressure curve is greater than the slope of the tube pressure line.

The limit of static stability then occurs when the slopes of the two curves are equal. For the particular case of a jet of air issuing from a reservoir at 5.16 atm. pressure, this condition gives (details are given in Appendix C):

$L/d < 1.8$ static stability

$L/d > 1.8$ static instability

where L is tube length and d tube diameter.

Experiments indicate that this is not quite correct. The experimental resonance tube was plugged with a tightly fitted wooden dowel and placed in the jet. The interesting results for a supersonic jet and for a periodic jet are shown in figure 6. The situation may be summarized as follows:

Periodic Jet: The bow shock system oscillates violently even for a tube of zero length (i.e. - the blunt body). In the experiment, intense high frequency noise was emitted as the shock system oscillated.

Supersonic Jet: The bow shock is stable for a tube of zero length. As opposed to the periodic jet, then, a tube and jet are required to form an unstable system. This is related to the fact that changes in the external flow are responded to by the tube only after a response time of 2L/a, the time necessary for a transit and return of the disturbance signal.

## The effect of separation distance on oscillation

Figure 7 shows the pressure response of the resonance tube as a function of nozzle-to-tube distance. The pressure response is taken as the maximum difference in pressure indicated by a transducer at the closed end. The regions of instability are clearly evident for the periodic jet.

Measurements of closed end temperatures as a function of separation[6,7] show a much stronger peaking. A change in the character of the external flow occurs with position, such that the strength of the internal shocks varies significantly. Thus, some positions may show strong pressure variation, but for an almost isentropic flow. In preparing the photographic data, positions without overtones were sought. At such

positions, the high speed films indicate precise periodicity.

The stability problem in the case of a straight supersonic jet has not been considered. It may be investigated, however, by using perturbation equations derived in Appendix I.

Influence of tube end shapes

The shape of the open end does not seem to affect the oscillation greatly. A plane flange (figure 15) was fitted to the tube. The pressure records made during oscillation were not different from those obtained for the unflanged case.

In another test, the flange was mounted while the experimental setup was located in a sound insulating enclosure (figure 17). The tube resonated nicely but the entire mass flow passed out the light duct, perpendicular to the tube axis, instead of flowing axially along the tube in the usual way. This was of course a result of the resistance to axial flow offered by the flange, compounded by the confining enclosure.

## IV THE SIMPLE TUBE EXCITED BY A PERIODIC JET

Beginning with the experiments of Hartmann, the periodic jet has been the prevalent means of excitation for resonance tubes.

Some data for this case are presented here. Special features of the flow are:

i) Pressure amplitude at the closed end is a larger multiple of the reservoir pressure than in the supersonic case.

ii) The time required for transition from outflow to inflow is somewhat shorter than in the supersonic jet case (e.g. 15% E vs. 24% E).

iii) During the transition to inflow, the nodal structure of the entering jet gives rise to a train of shocklets entering the tube (see figure 8-2 and Fam's shadowgraphs).

iv) Distinct resonance positions correspond to the converging portions of the jet cells.

Figure 8 shows timed shadowgraphs of the external flow. Transducer pressure records appear in figure 9.

8-1: Beginning of the temporarily steady outflow. A secondary shock is moving outward from the tube toward the main collision system.

Figure 8: External flow shadowgraphs - periodic case

separation: 1.600 in.
reservoir pressure: 60.0 psig
pressure ratio: 5.08
period: B = 7.31 ms

8-2: Transition to inflow. Pressure nodes are visible downstream of the main jet shock.

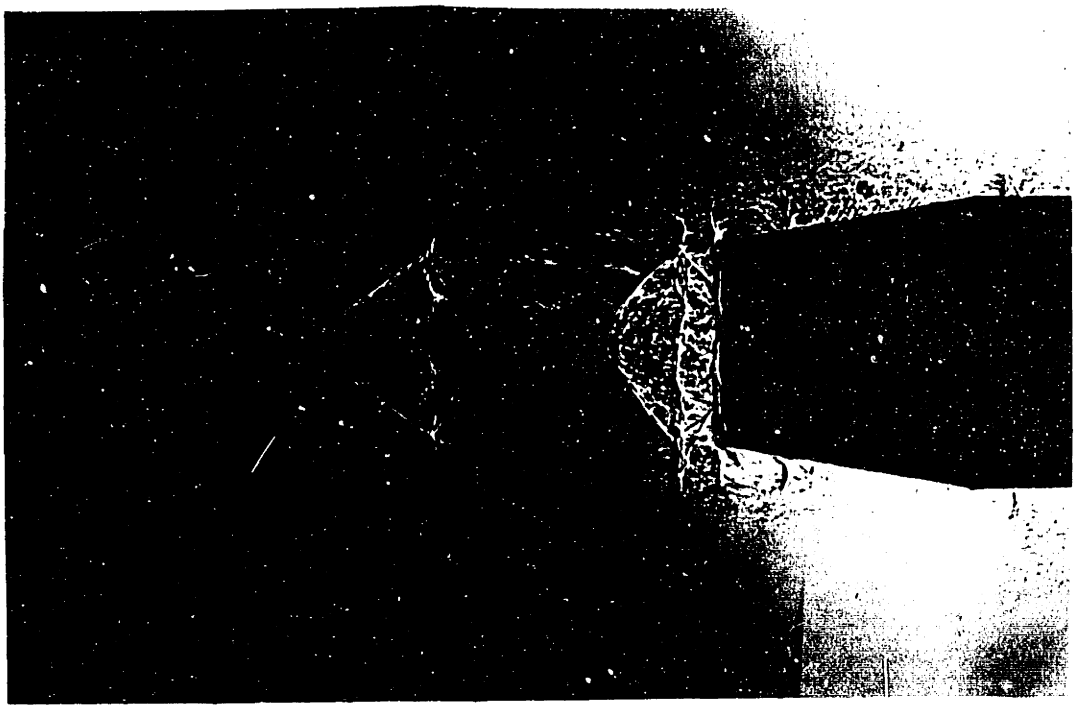

8-3: Temporarily steady inflow.

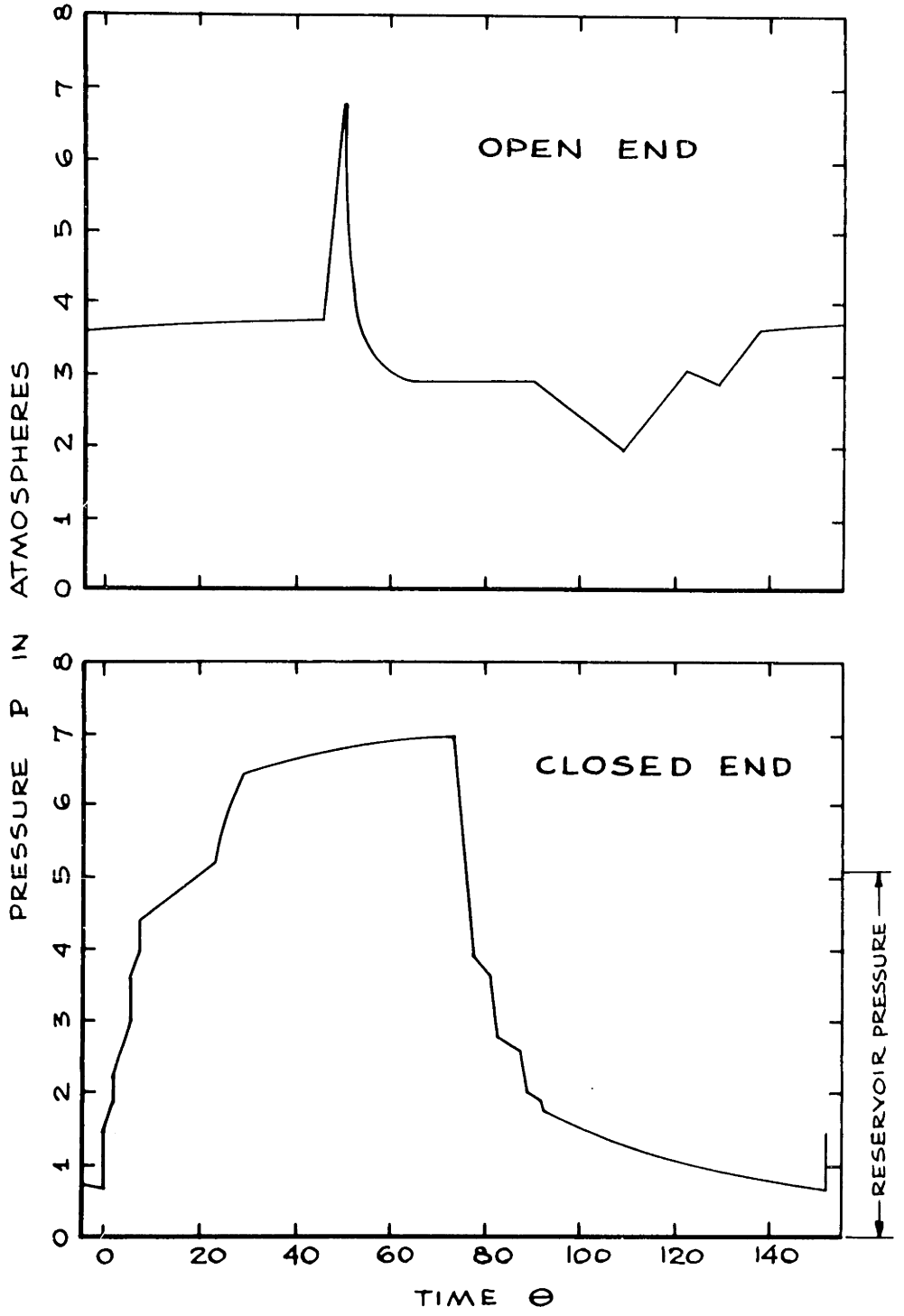


FIG. 9: PRESSURE RECORDS - PERIODIC CASE

## V THE SIMPLE TUBE EXCITED BY A SUPERSONIC JET

Shadowgraphs and pressure records show that the flows for this case are simpler than for the tube excited by a periodic jet. For this reascn, the analysis has been restricted to the supersonic case.

Internal flows have been analyzed by the application of simple boundary conditions at the open end. Results are presented for two cases.

i) The tube is ideally cooled, sc that the mean stagnation temperature within the tube does not rise above environment temperature.

ii) The tube is insulated, so that a considerable heating of the indigenous fluid obtains.

Sequential shadowgraphs of the external flow appear in figure 10.

### The problem of interaction between tube flow and jet

As previously mentioned, the internal flow is mathematically determinate if sufficient information can be supplied about the interactions at the tube open end. The unsteady external flow is so complicated, however, that a complete solution is probably proscribed. However, two approximate approaches have been formulated:

been formulated:

i) Integral equations have been written for the unsteady flow of a jet. By assuming certain radial distributions for the velocity and pressure, and applying continuity and momentum theorems for a control volume extending across the jet, one-dimensional equations are obtained. Because these equations combine the effects of radial and longitudinal motion, they are designated dyadic jet equations. Because the application of these equations required excessive computation, they were not used. The derivation and two test solutions are presented in Appendix I.

ii) Boundary conditions for the internal flow have been formulated. These are derived in Appendix D and presented in the form of pressure-velocity boundary state curves (figure 19). The derivation depends on the fact that the transition to inflow takes place slowly. Thus, during this portion of the flow, unsteady acceleration terms may be neglected, and the flow at the mouth is taken as quasi-steady. In this connection, comparison should be made between figures 6-1 (stagnating jet, steady flow) and 10-8 (stagnating jet, quasi-steady flow). The agreement is striking. Further, the validity of simple boundary conditions depends upon the insensitivity of the internal tube flow to the details of external flow. Such insensitivity was demonstrated in the aforementioned flange experiment.

Wave diagram for an ideally cooled tube

In order to construct a wave diagram for the flow, it is then necessary to supply a reasonable set of initial conditions. The following initial state is

taken: Fluid in the tube is at rest, with the full jet mass flow instantaneously entering the tube with a standing normal shock at $X = 0$, the tube mouth. There are thus two shocks, the stationary normal shock at the mouth, and the traveling shock which separates the full jet inflow from the region of zero velocity. The contact interface between extraneous and indigenous fluid is taken as being without entropy discontinuity.

Heat transfer from the gas to the tube walls is handled according to a very simple model. Since, for periodic oscillation, entropy generation by shock waves is just balanced by entropy removal through heat transfer, there is no net entropy generation over a cycle. All shocks are therefore treated as isentropic, resulting in considerable lessening of computation. Since the shocks are of moderate strength, the error introduced into the dynamics is small.

The characteristic equations for one-dimensional inviscid flow are:

$$(U + \frac{2}{k-1} A)_\theta + (U+A)(U + \frac{2}{k-1} A)_X = 0 \qquad (5.1)$$

$$(U + \frac{2}{k-1} A)_\theta + (U-A)(U - \frac{2}{k-1} A)_X = 0 \qquad (5.2)$$

where U and A are fluid velocity and scund speed, both normalized with respect to the sound speed in the correctly expanded jet, and $\Theta$ and X are dimensionless time and distance.

For isentropic shocks, the characteristic of opposite family is invariant across the shock. That is, the shock polar is just a characteristic line.

The first wave diagram is computed for the case in which the tube is ideally cooled: That is, there has been no accumulation of entropy, and the time mean stagnation temperature at all stations in the tube turns out to be just the stagnation temperature of the jet. Since there is no entropy discontinuity in the internal flow, the wave diagram construction is quite simple.

Using the aforementioned initial conditions, the computed oscillation becomes almost perfectly periodic after three cycles. The wave diagram (ideally cooled case, jet Mach Number = 1.92) is shown in figure 11. The pressure history from this diagram is compared with the experimental data (for a well-cooled tube) in figure 12.

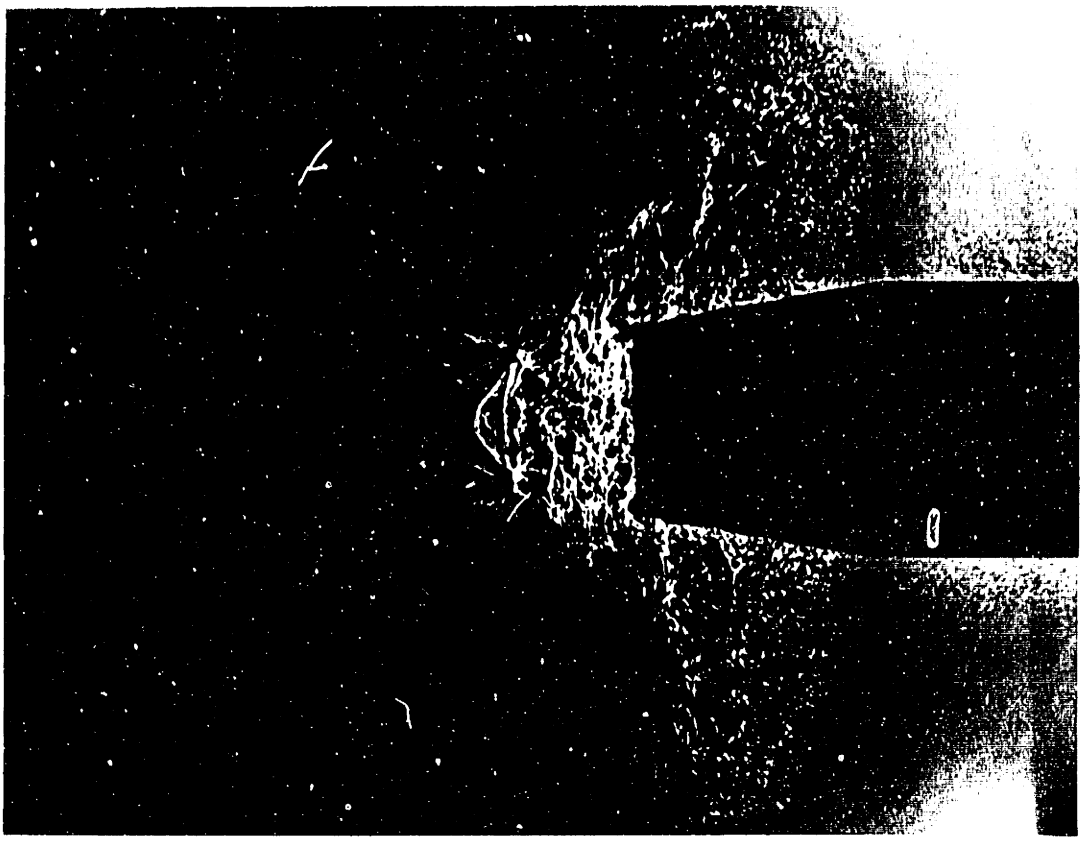

10-1 (.13 ms): Transition to outflow. The main shock has just emerged from the tube mouth, generating the spherical atmospheric shock visible in the left hand corners.

Fig. 10: External flow shadowgraphs - supersonic case

Times given are based on a reference zero corresponding to the incidence of the outgoing shock at the open end.

separation: 1.155 in.
reservoir pressure: 85.0 psig
pressure ratio: 6.83
period: B = 6.80 ms


10-2 (.17 ms): An outflow jet is visible. A second shock is forming near the tube mouth.

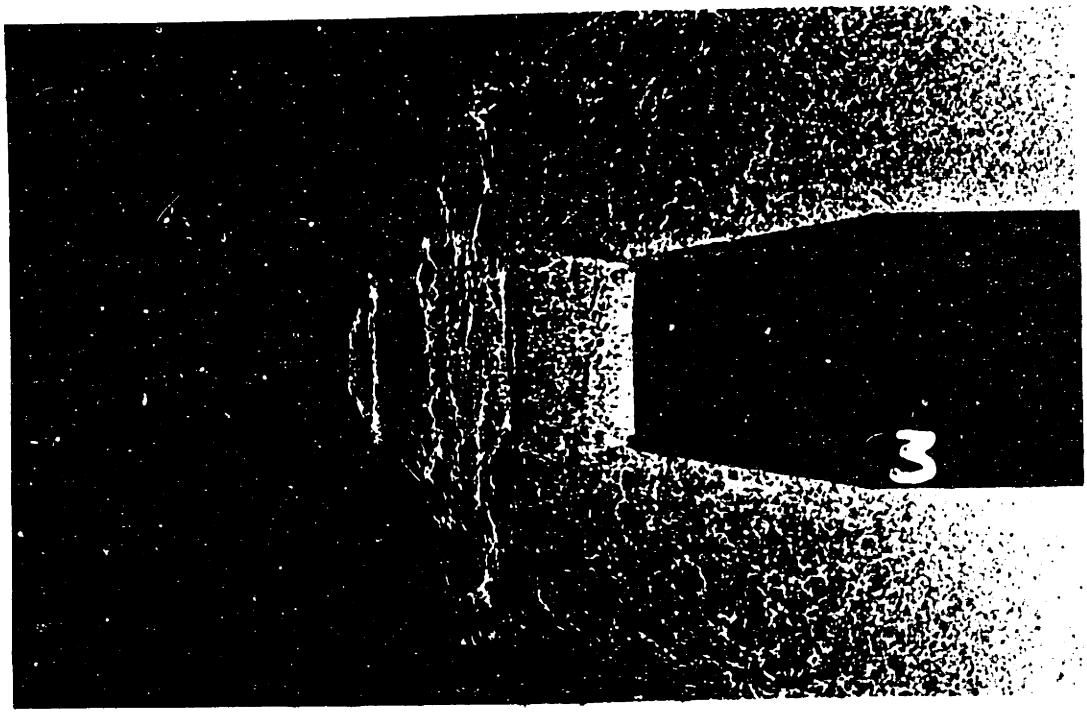


10-3 (.34 ms): Outflow almost fully established. The appearance of corner nodes in the tube mouth shadow indicates overpressure.

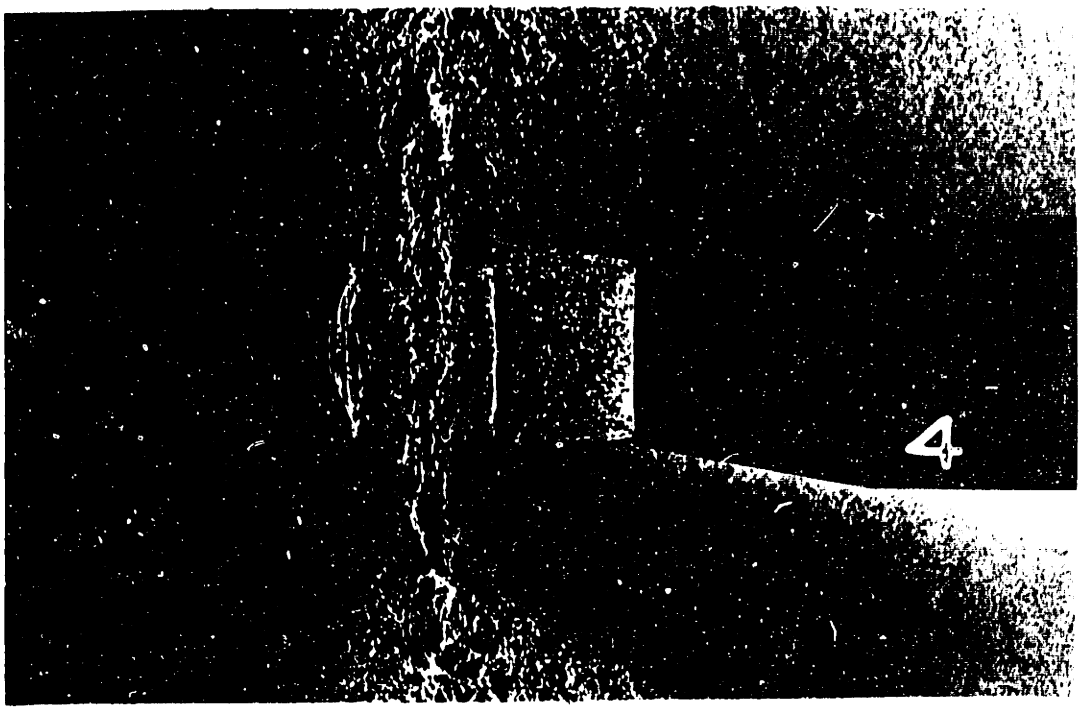


10-4 (.44 to 2.69 ms): Temporarily steady outflow. At the slope discontinuity in the jet shock the condition of equal turning angles must be satisfied.

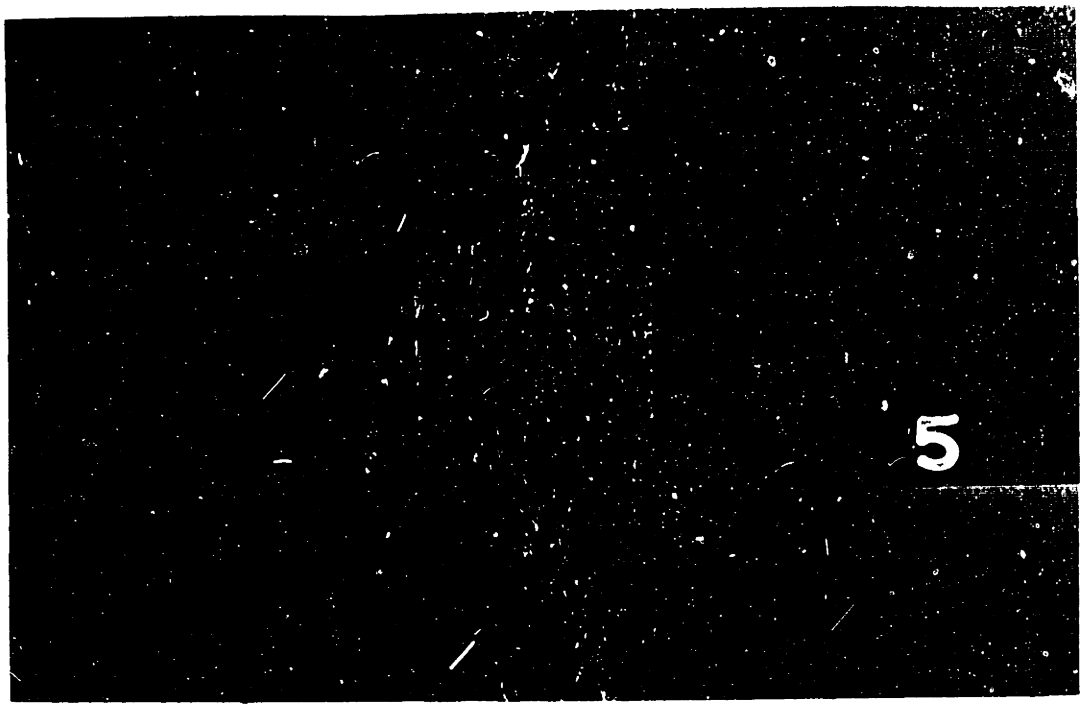


10-5 (3.00 ms): Outflow has begun to weaken.

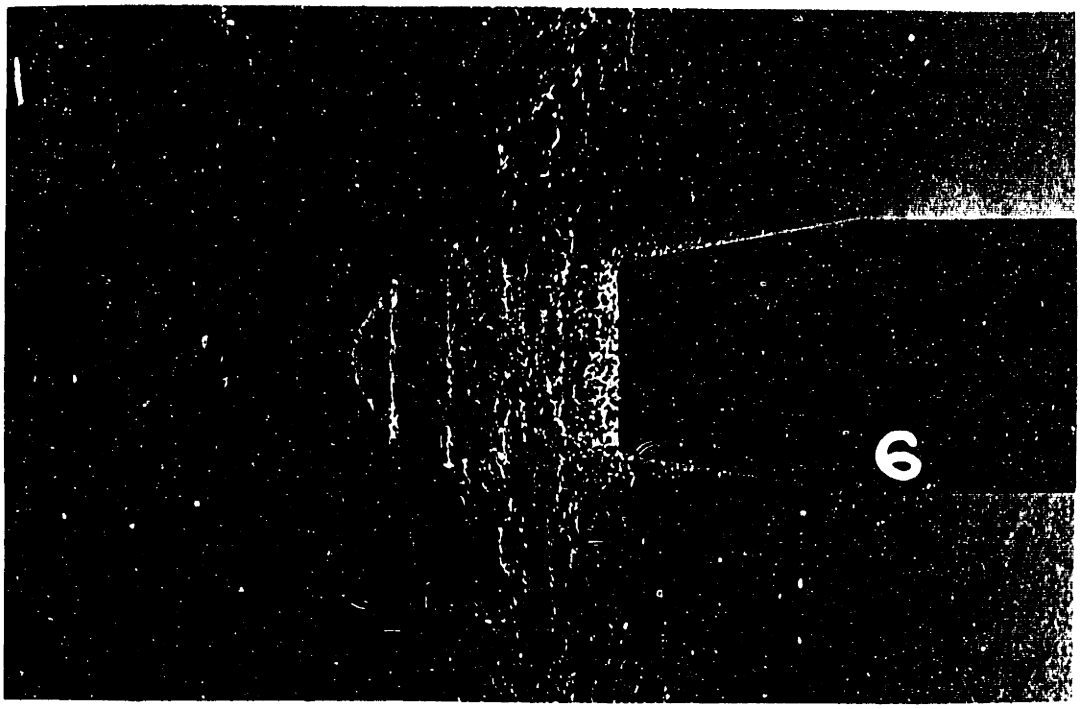


10-6 (3.14 ms)

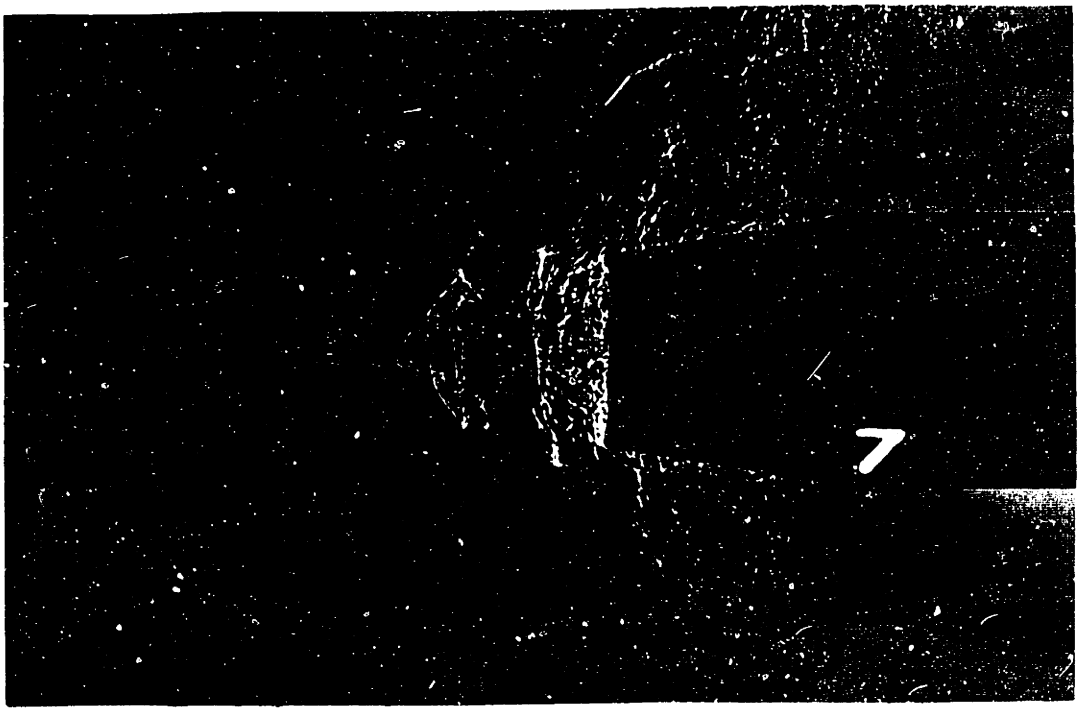


10-7 (3.59 ms)

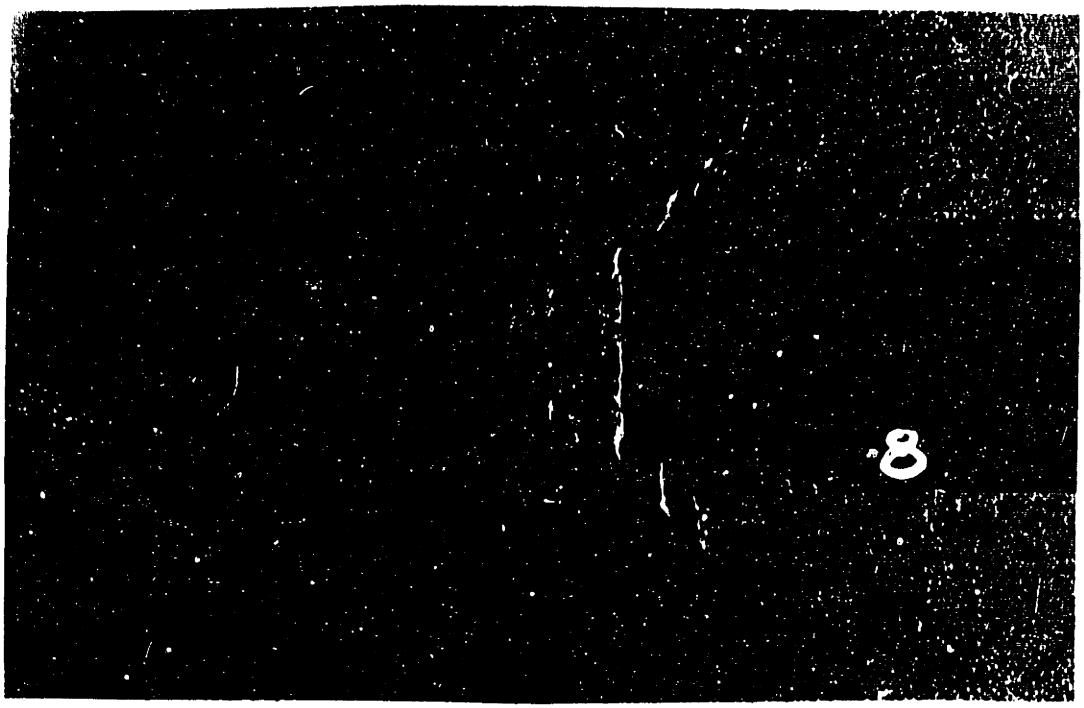


10-8 (3.76 ms): Ey comparison with figure 6-1, this appears to represent stagnation at the tube mouth.

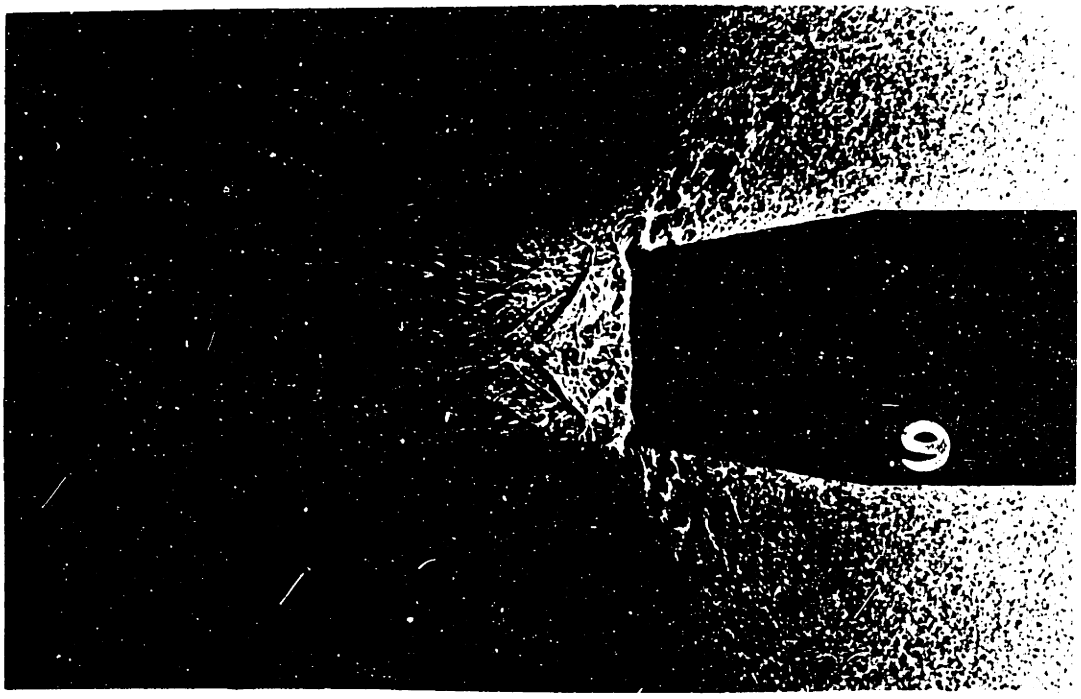


10-9 (4.11 ms): The open centered shock is slowly moving toward the tube mouth.

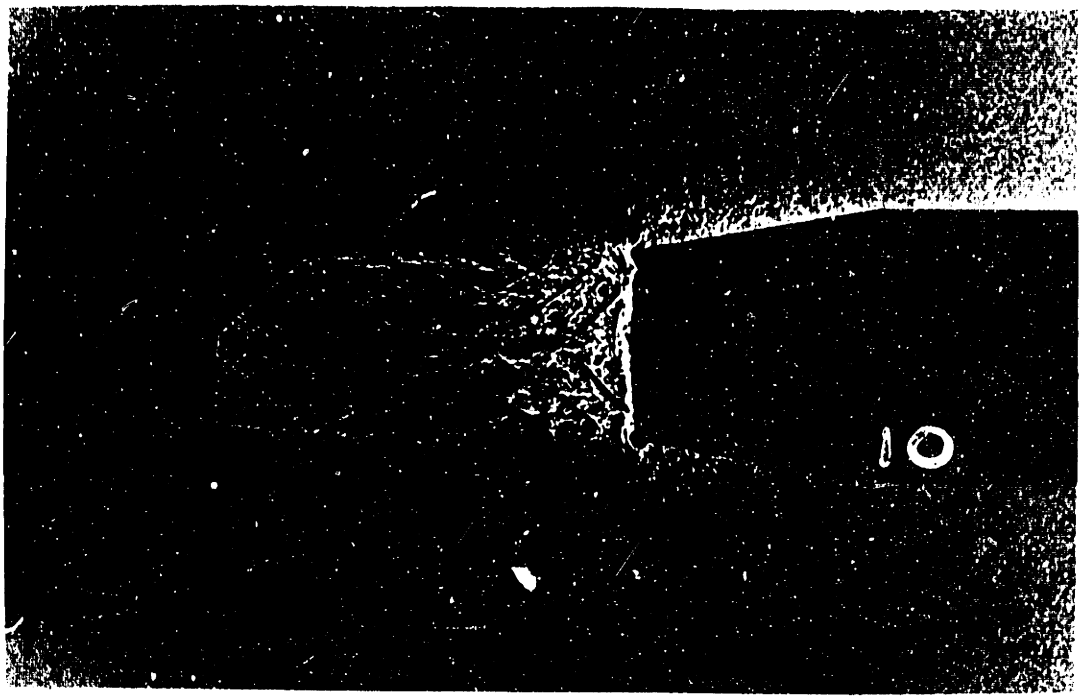

10-10 (4.22 ms)

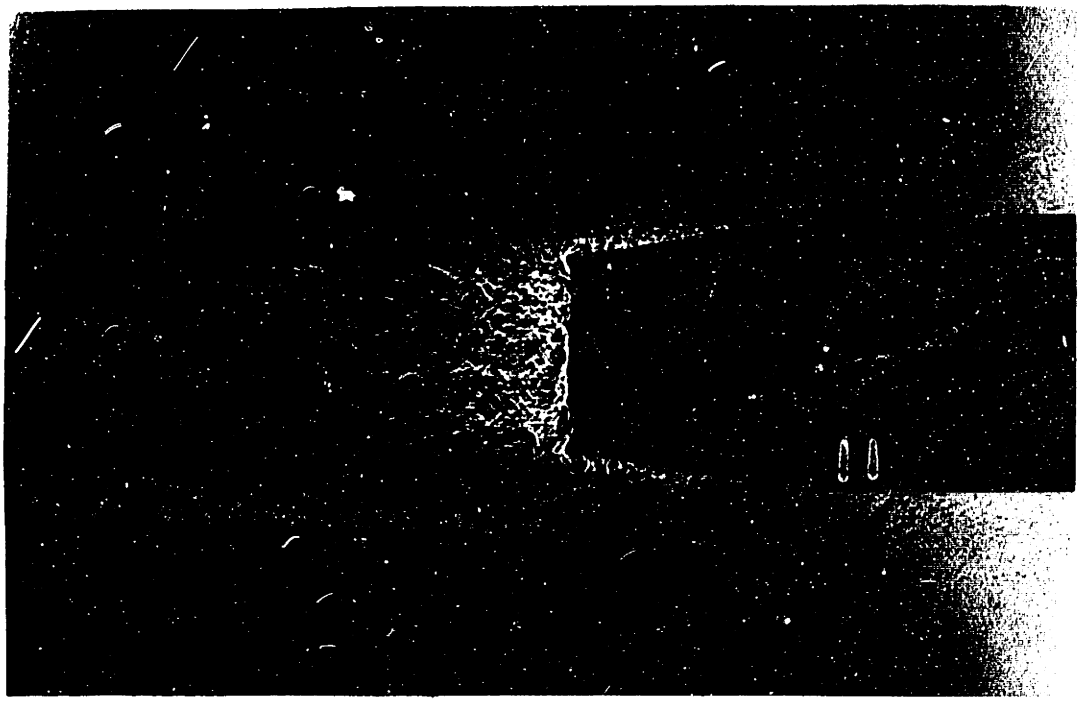

10-11 (4.30 to 6.80 ms): Temporarily steady inflow. Corner nodes again indicate overpressure.

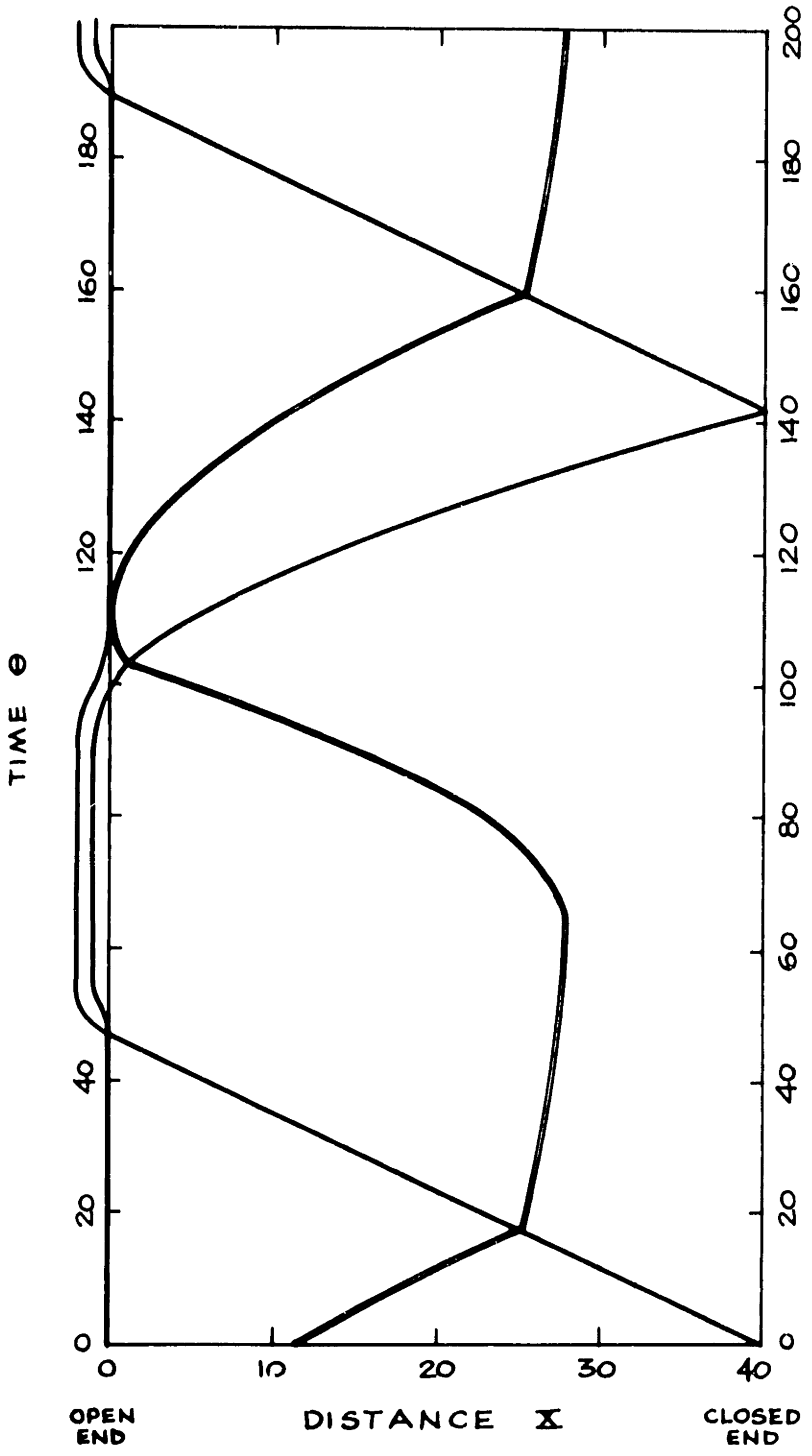


FIG. 11: WAVE DIAGRAM FOR AN IDEALLY COOLED TUBE

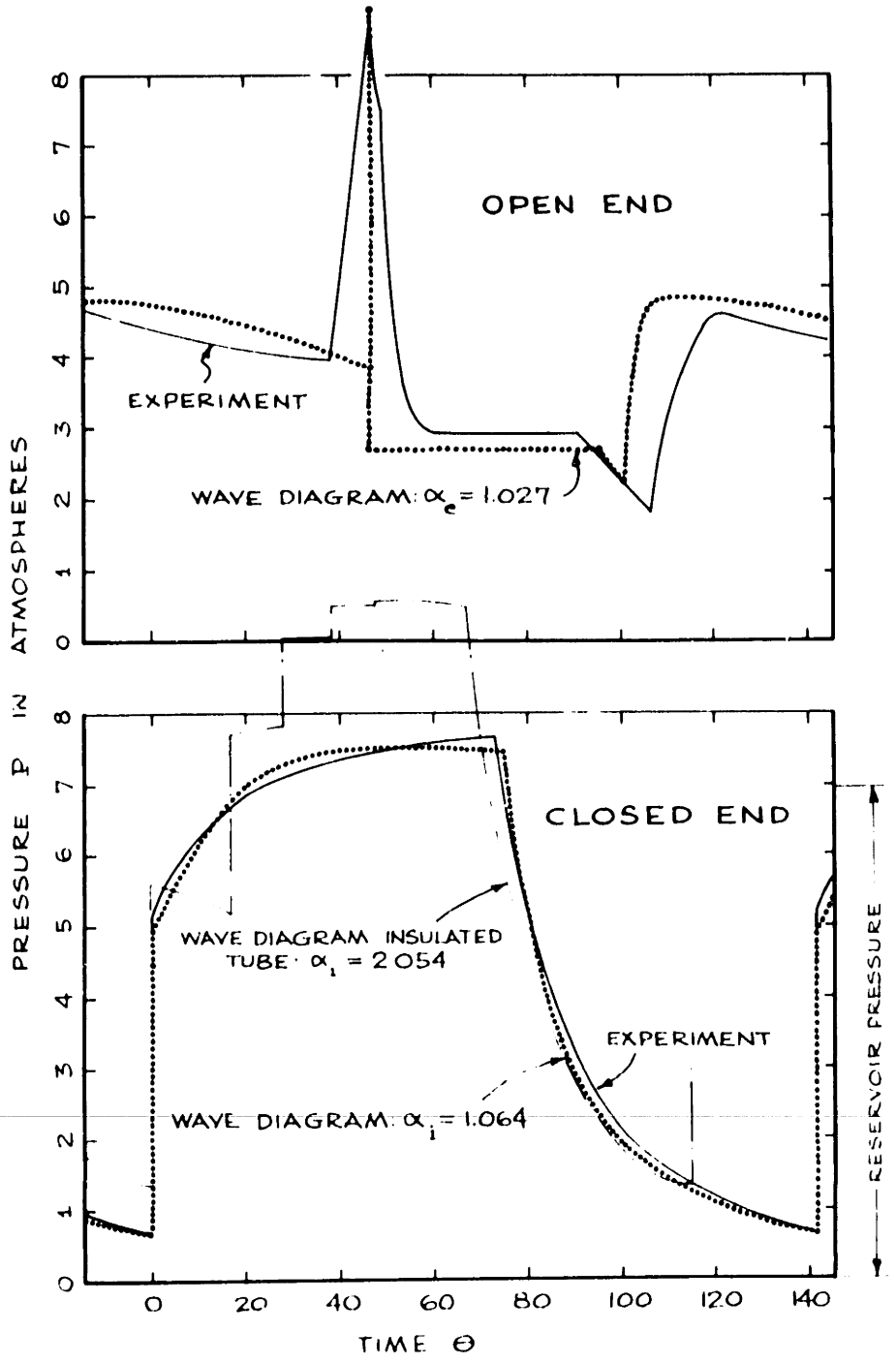


FIG 12: PRESSURE RECORDS - SUPERSONIC CASE

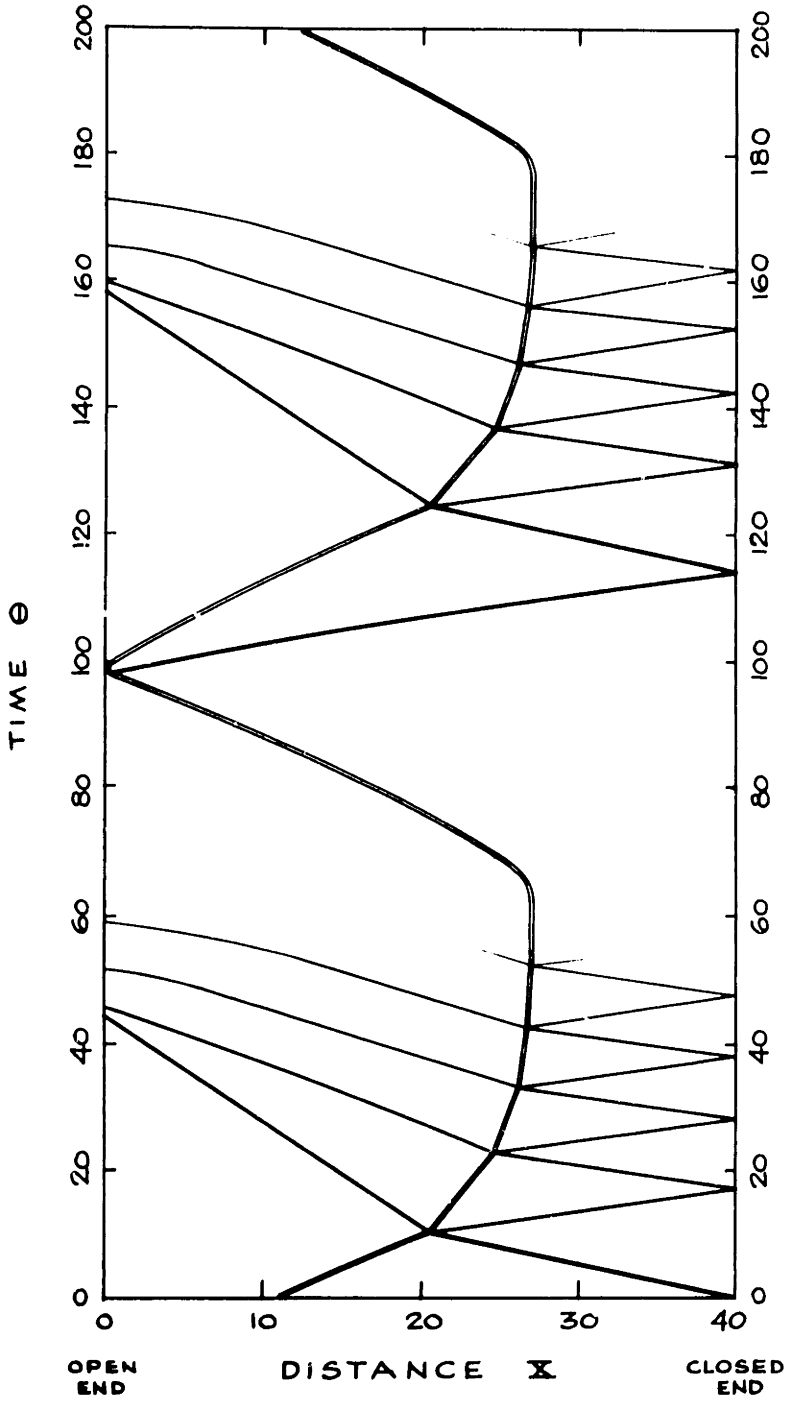


FIG. 13: WAVE DIAGRAM FOR AN INSULATED TUBE

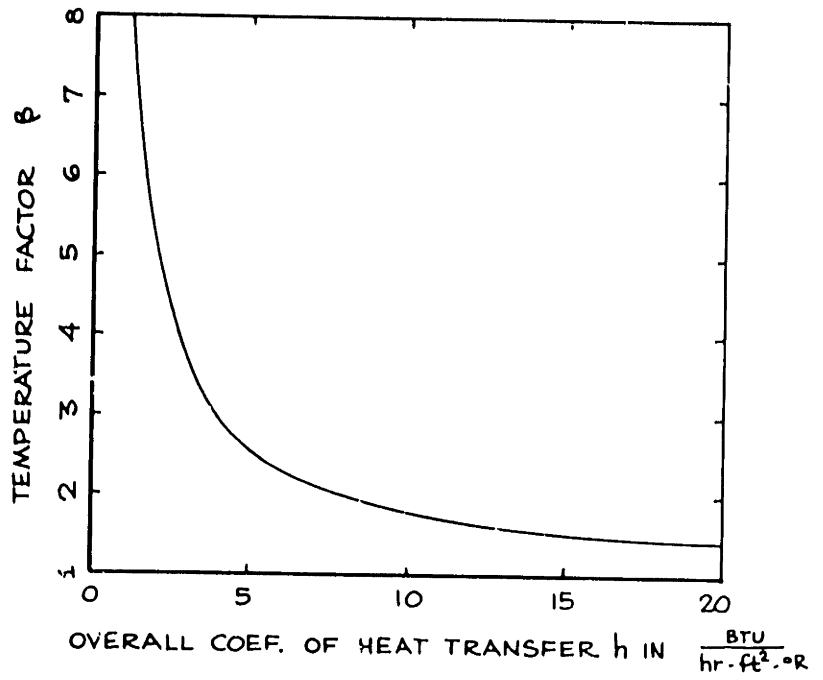


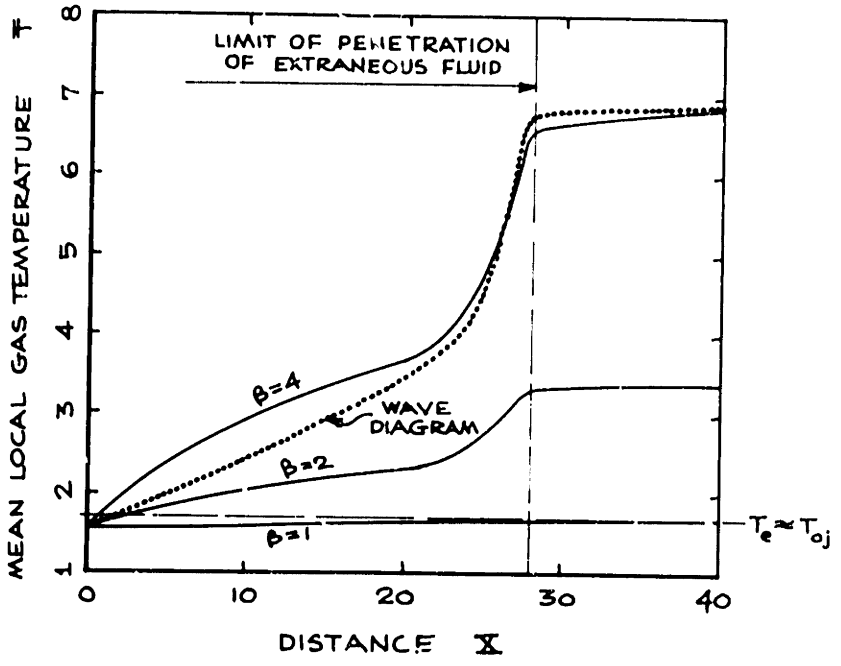


FIG 14: COMPUTED TEMPERATURE DISTRIBUTIONS

Wall temperature distribution

An estimate of the tube wall temperature is obtained by assuming the dynamics (pressure and velocity) for an insulated tube to be the same as for the perfectly cooled case. The temperature of the indigenous fluid is taken as increased by a constant factor $\beta$. The time mean temperatures and the time mean stagnation temperatures at fixed X are then determined, for various positions along the tube, from the wave diagram. These values are of the form:

$$\overline{T} = C_1 + C_2\beta \tag{5.3}$$

$$\overline{T}_o = C_3 + C_4\beta \tag{5.4}$$

where the C's vary with the station. T is absolute dimensionless temperature, normalized with respect to temperature in the correctly expanded jet.

In addition, the twice averaged (space and time)

indigenous temperature has the form:

$$\bar{\bar{T}}_i = c_5 \beta \tag{5.5}$$

The entropy generation is assumed independent of $\beta$. If thermal storage in the tube wall is neglected, the heat generated may be balanced against the heat transfer as:

$$m_i \bar{\bar{T}}_i (\Delta s)_{cycle} = hB\pi d \int_0^L (\bar{T}_{oi} - T_n) dx \tag{5.6}$$

where $m_i$ is the mass of indigenous fluid, $h$ is the overall coefficient of heat transfer, and $T_n$ is the environment temperature. There results an equation for $\beta$, the unknown, as a function of $h$.

$$\beta = f(h) \tag{5.7}$$

The details of this operation are carried out in Appendix E. Then for a given $h$, $\beta$ and consequently the mean temperature can be determined at any $X$. Resulting temperature distributions are presented in Figure 14.

Heat release efficiency

By comparing the heat release $m_i \bar{\bar{T}}(\Delta s)$ with the kinetic energy discharged by the jet during one cycle of operation, an "efficiency" for heat generation may be computed. For the case considered (ideally cooled tube), this is about one percent.

Wave diagram for an insulated tube

The case in which a very strong entropy discontinuity exists at the interface between indigenous and extraneous fluid is now considered. In particular, the indigenous fluid is taken to have uniform entropy such that:

$$\frac{\alpha_i}{\alpha_e} = 2 \qquad (5.8)$$

where $\alpha^2 = P^{1/k}/G$ is a constant for isentropic flow. The condition of equal pressures at the interface gives:

$$\beta = \frac{T_i}{T_e} = \frac{P_i/G_i}{P_e/G_e} = \frac{G_e}{G_i} = \frac{P_e^{1/k}/\alpha_e^2}{P_i^{1/k}/\alpha_i^2} = \frac{\alpha_i^2}{\alpha_e^2} = 4$$ *

Conditions for characteristics incident on the entropy discontinuity are developed in Appendix F.

The boundary conditions are unchanged, since they relate only to extraneous fluid. Initial conditions are taken from the perfectly cooled tube at the instant the shock is incident on the closed end: identical U(X) and P(X), but with T(X) increased by a factor of four for the indigenous fluid only.

The periodic solution for a jet Mach Number of 1.92 is presented in figure 13. Additional shocks resulting from reflections at the contact interface are present. The period is, not surprisingly, less than that of the ideally cooled tube. The outflow is accelerated to supersonic speed by secondary shocks.

*The mean temperature of extraneous fluid is about equal to jet stagnation temperature, say 540 $^{o}$R. The mean indigenous temperature is then about 2160 $^{o}$R for this case.

The time mean temperature is plotted in figure 14. The distribution obtained is not greatly different from that given by the heat transfer analysis. The entropy generation per cycle, $\Delta S/R$, is .070, as opposed to .075 for the perfectly cooled case.

## Discussion of wall temperature distribution

Sprenger[6] and Howick and Hughes[7] show temperature distributions for the wall of a tube excited by a periodic jet. The distribution given here differs from that of Sprenger and most of those of Howick and Hughes. Aside from the fact that the excitation means are dissimilar, the effect of axial conduction in the tube wall is to produce distributions more like the experimental ones.

Further, for tube walls with finite heat capacity (as opposed to the idealized case considered in the computations), axial conduction is supplemented by fluid heat transport.

# VI CONCLUSION

## On the attainability of high temperature

The presence of a continuous positive entropy gradient is known to inhibit the steepening of compression waves. Shapiro[19] has considered the effect of this inhibition on the heating of resonance tubes.

The assumed model, in which the entropy of the indigenous fluid is uniform, is apparently satisfactory for moderate heating. However, entropy gradients may arise from the following:

i) Different path lines traverse shocks of different strengths.

ii) Different path lines are subject to different entropy reductions by heat removal.

Considering the wave diagram for an insulated tube as a guide, it is decided that effect (i) is not present. Effect (ii) is present to some degree. The time mean temperature for all indigenous fluid particles is about the same. However, for tubes of finite wall thickness, the particles nearer the open end are exposed to a lower mean wall temperature, and are thus subject to greater heat transfer. This effect is just parallel to that of axial conduction.

In spite of the foregoing, it is anticipated that high temperatures are attainable. Careful experiments with very well insulated tubes remain to be performed. In addition, the behavior of an adiabatic tube may be theoretically tested by using the previously developed boundary conditions in conjunction with a computer solution for the internal flow. For such a solution, the isentropic shock simplification must of course be dropped.

Geometric factors

The theory presented for tubes excited by a supersonic jet shows no effect on the dimensionless variables from changes in the tube diameter. Possible effects from changes in tube length are:

i) Changes in shock strength due to change in the available distance for compression wave steepening.

ii) Real effects consisting in inhibition of steepening by entropy gradient, decay of shock strength, and heat transfer.

Effects (i) and (ii) are generally opposed. The optimum length for temperature increase probably depend on the degree of insulation. The figure of 34:1 obtained by Sprenger serves as a guide.

## Possible future experiments

Tests of very well insulated tubes and tapered tubes would be interesting.

For future experiments, a superior means for obtaining accurately timed shadowgraphs is available. The light source shown in figure 18 can be triggered by a relatively weak signal, as from a crystal microphone. In order to obtain flashes timed in relation to a particular cycle, it is thus adequate to employ a movable microphone near the tube mouth. For such an arrangement, the spherical shock visible in figure 10 (frame 1) will act as a very clean signal. Then for microphone movement along a radius drawn from the tube mouth, and sufficiently far from the mouth so that the shock speed is about constant,

$$\Delta r = a\,\Delta t$$

$\Delta r$ is the distance moved by the microphone, and $\Delta t$ the time interval between positions.

Electronic variable delays can of course be constructed, but the above method is far cheaper and generally more accurate. Using the method in conjunction with transparent wall tubes, precise experimental

wave diagrams can be constructed.

Noise hazard

The emitted sound is intense. Personnel within about one hundred feet of the apparatus may suffer severe discomfort if their ears are unprotected.

General comments

Multiple internal shocks may appear from two sources: the refocusing of the jet (periodic case), or, as shown in the wave diagram for an insulated tube, collision of a shock with the discontinuity interface (both cases). The interface itself may be visible in internal shadowgraphs.

The heat release has been assumed to result exclusively from dissipation within shock waves. Boundary layer heating[22] and turbulent decay heating[6] are also present. That the latter effects are normally small is indicated by the very slight heating produced in tubes excited by subsonic jets. They may become very significant, however, as in the accidental introduction of solder particles by Sprenger.

This thesis has attempted to describe all of the

## APPENDIX A: LIST OF SYMBOLS

| | |
|---|---|
| a | subscript denoting reference state in correctly expanded supersonic jet. |
| a | sound speed. |
| A | dimensionless sound speed = $a/a_a$. |
| $\alpha$ | isentropic constant. |
| B | oscillation period. |
| $\beta$ | heating factor. |
| $C^+$ | dimensionless Riemann Invariant. |
| $C^-$ | dimensionless Riemann Invariant. |
| d | tube diameter. |
| $d^*$ | jet diameter. |
| D | dimensionless jet diameter = $d^*/d$. |
| e | fraction of full jet mass flow = $GU/M_a$. |
| $\rho$ | fluid density. |
| G | dimensionless fluid density = $\rho/\rho_a$. |
| h | overall coefficient of heat transfer. |
| j | flow impulse = $p + \rho u^2$. |
| J | dimensionless impulse = $P(1 + kM^2)$. |
| k | ratio of specific heats. |
| L | tube length. |
| m | mass. |
| M | Mach Number = U/A. |
| N | dimensionless radial distance = $2r/d^*$. |

| | |
|---|---|
| o | subscript denoting stagnation conditions. |
| p | fluid pressure. |
| P | dimensionless fluid pressure = $p/p_a$. (pressure in atmospheres) |
| Q | quantity of heat. |
| r | radius from the jet centerline. |
| R | gas constant. |
| s | specific entropy. |
| t | time. |
| T | dimensionless absolute temperature. |
| $\Theta$ | dimensionless time = $a_a t/d$. |
| u | axial velocity. |
| U | dimensionless axial velocity = $u/a_a$. |
| v | radial velocity. |
| $v_1$ | radial velocity at jet boundary. |
| V | dimensionless radial boundary velocity = $v_1/a_a$. |
| x | longitudinal distance from the tube open end. |
| X | dimensionless longitudinal distance = $x/d$. |

## APPENDIX B: DESCRIPTION OF APPARATUS

1. Stainless steel resonance tube (figure 15).

2. Brass sonic nozzle (figure 15).

3. Brass supersonic nozzle, M = 1.92 (figure 15).

4. Flash lamp driver (figure 18). The xenon filled FX-2 lamp was covered with electrical tape in which a 1/64 inch diameter hole was pierced. Lamps of the type used are described in ref. 1.

5. Stroboscopic flash lamp driver: Edgerton, Germeshausen, & Grier, type 501, serial no. 26. The FX-21 lamp was covered with a taped slit 1/16 inch in width, such that the slit was perpendicular to the lamp axis.

6. High speed camera: Wollensak Fastax 16 mm, model W163269, serial no. 16-158, driven by Wollensak Goose power unit.

7. Oscillator: Hewlett-Packard wide range model 200 CD, serial no. 6189.

8. Oscilloscope: DuMont model 304-A, serial no. 7AA95.

9. Quartz crystal transducer, SLM model EPI-114 with piezo-calibrator.

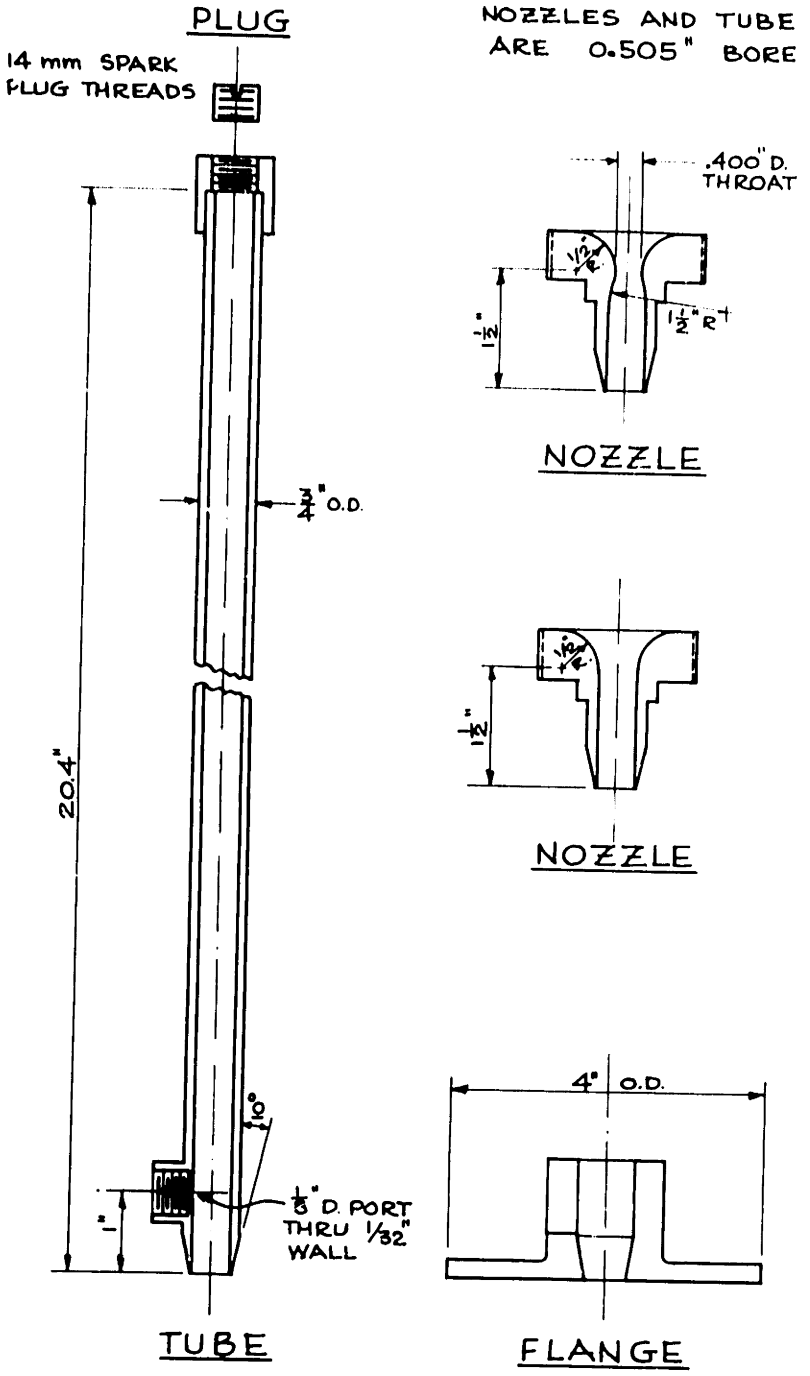


FIG. 15: RESONANCE TUBE AND ACCESSORIES

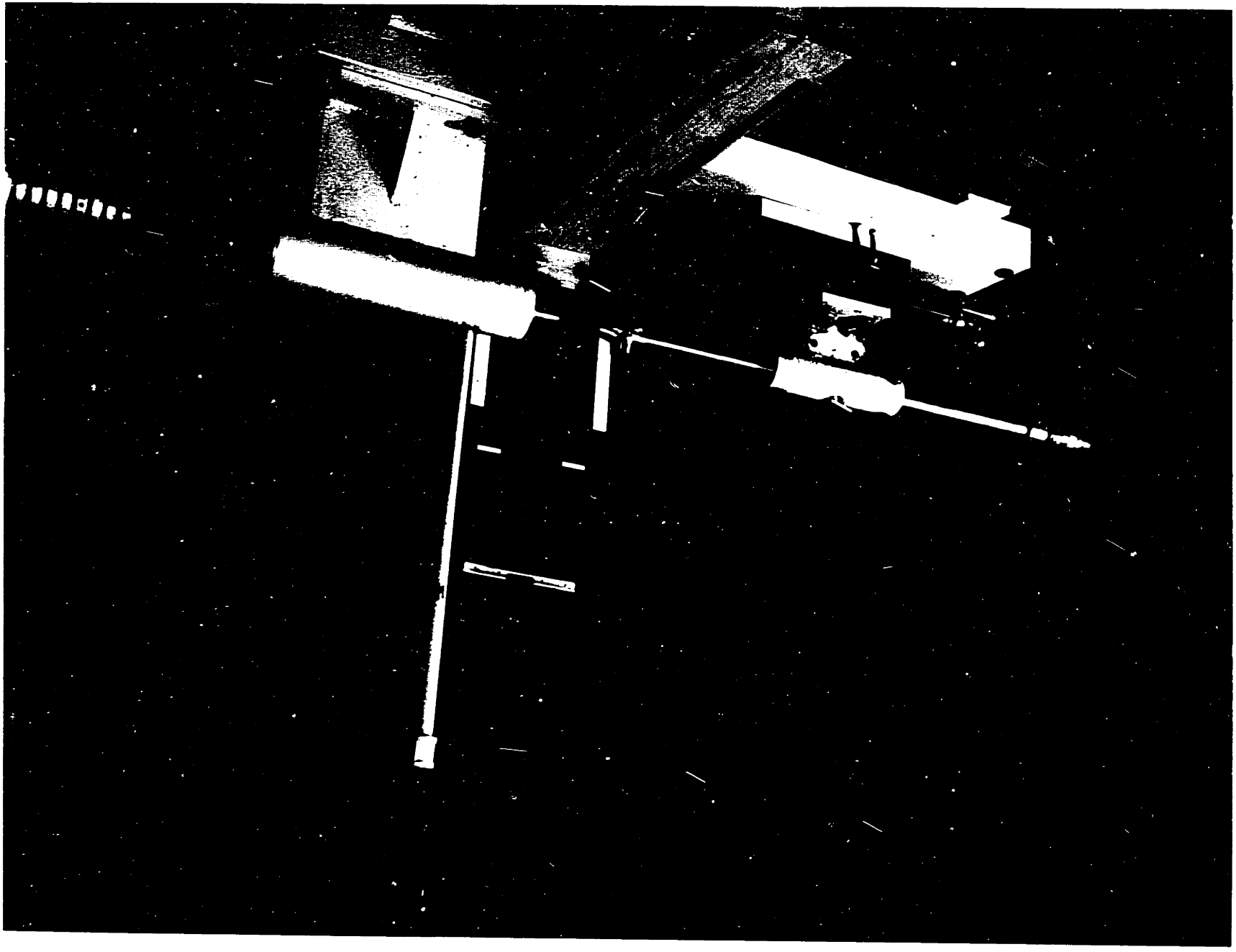

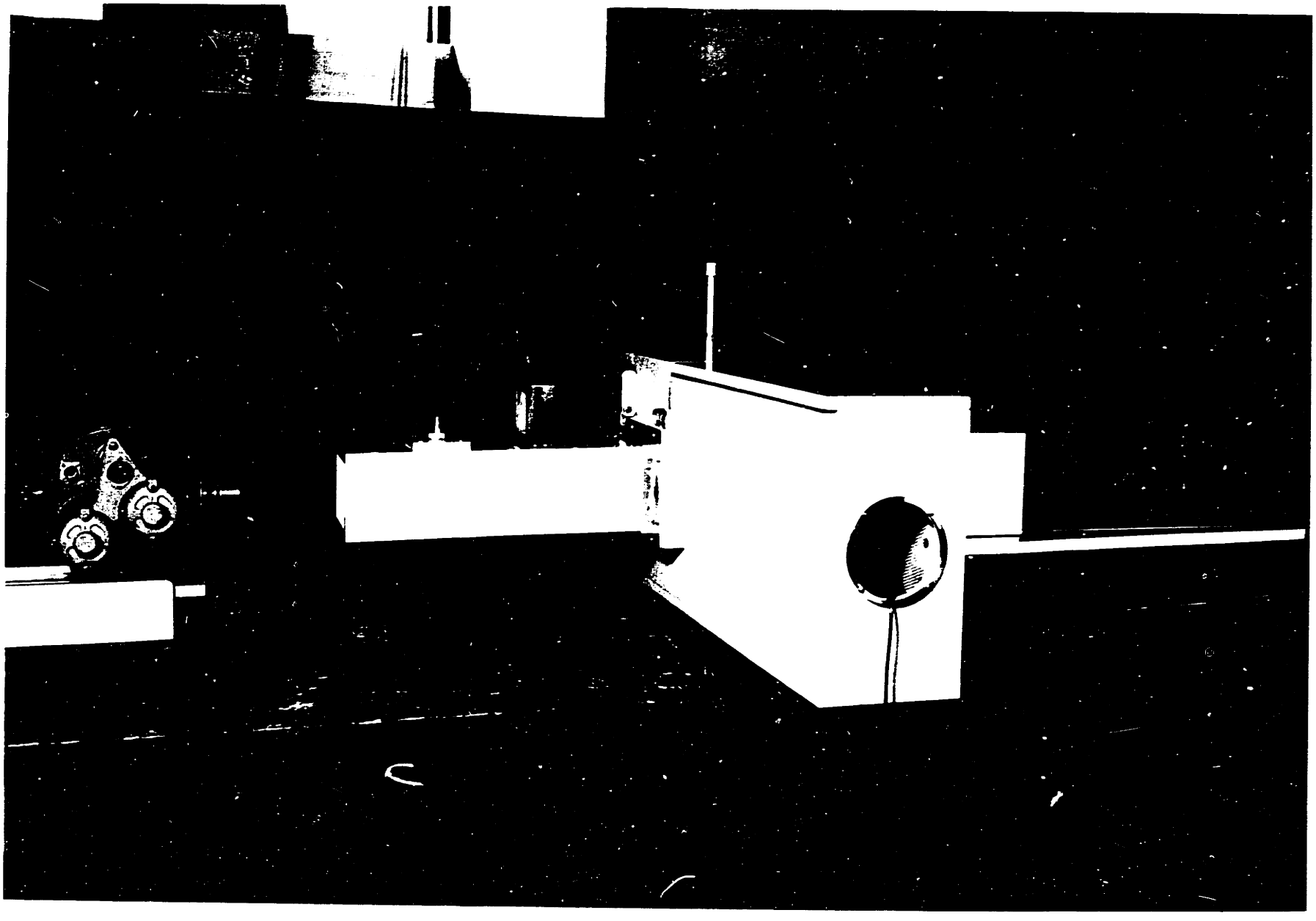

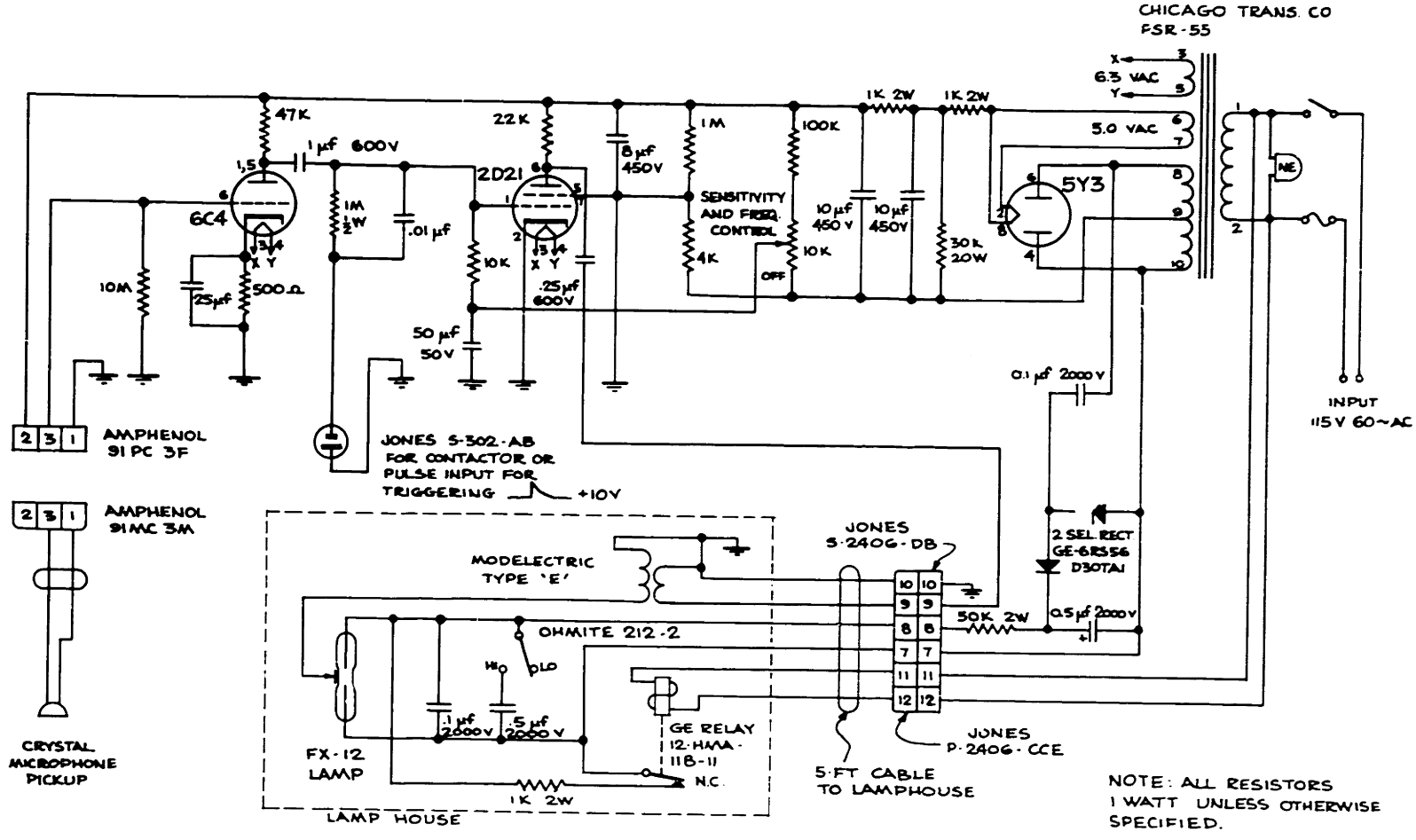


FIG. 18: LIGHT SOURCE WIRING DIAGRAM

## APPENDIX C: SIMPLIFIED MODEL OF THE STABILITY LIMIT

Reference is made to figure 5. For isentropic compression of the tube fluid:

$$pV^k = \text{constant}$$

where $V = (L-x)\,\pi\, d^2/4$, the gas volume. Then

$$p(L-x)^k = p_{oe}L^k = \text{constant}$$

$$p(1-x/L)^k = p_{oe}$$

For small $x$, approximately

$$p(1-kx/L) = p_{oe}$$

Differentiating with respect to $x$:

$$\frac{dp}{dx}(1-kx/L) - \frac{kp}{L} = 0$$

At $x = 0$, $p = p_{oe}$ and the slope is

$$\frac{dp}{dx} = k\frac{p_{oe}}{L}$$

In dimensionless form, using $x/d = X$ and $p/p_a = P$:

$$\frac{dP}{dX} = k\frac{P_{oe}}{L/d} \qquad (C.1)$$

which states that the "spring constant" of a tube is inversely proportional to its length. The slope of the stagnation pressure curve is taken directly from the data of Hartmann and Lazarus. For the particular case of a reservoir pressure of 5.16 atm., from their figure 7c, at the most critical point :

$$\frac{dP_o}{dX} = 6.39$$

$$P_{oe} = 2.50$$

The limit of static stability is given by equality of slope:

$$\frac{kP_{oe}}{L/d} = k\,\frac{2.50}{L/d} = 6.39$$

or, using $k = 1.400$:

$$L/d = 1.8$$

## APPENDIX D: BOUNDARY CONDITIONS AT THE OPEN END

Conditions are to be established for the particular case of jet Mach Number 1.92, L/d = 40.

It should first be noted that some phases of the cycle are autonomic; that is, external conditions do not determine the solution of internal flow. For example, sonic or supersonic outflow proceeds quite independently of the jet motions, so long as the collision system stands away from the mouth of the tube.

Furthermore, during all phases of the internal flow, at least one characteristic $C^-$ reaches the open end from the tube interior:

$$U - \frac{2}{k-1}A = C^- \qquad (D.1)$$

Here, $U = u/a_a$ and $A = a/a_a$ are dimensionless velocity and sound speed. The reference sound speed $a_a$ is that for the correctly expanded jet. $C^-$ is known, and $U$ and $A$ are the required unknowns at the open end. An additional relation is then needed between $U$ and $A$.

It is then necessary to find a state equation relating the sound speed $A$ to density, pressure, and temperature.

Define

$$G = \rho/\rho_a \qquad \text{dimensionless density}$$

$$P = p/p_a \qquad \text{dimensionless absolute pressure}$$

$$\hat{T} = T/T_A \qquad \text{dimensionless absolute temperature}$$

where the reference state denoted by subscript a is for the correctly expanded jet. The flex over the T is immediately dropped, with the understanding that "T" will always refer to dimensionless temperature. The perfect gas equation of state is assumed to hold; it is:

$$P = GT \tag{D.2}$$

For isentropic processes:

$$\frac{P^{1/k}}{G} = \alpha^2 = \text{constant} \tag{D.3}$$

where k is the ratio of specific heats.

The sound speed is given by:

$$A^2 = T \tag{D.4}$$

The above equations yield:

$$A = \alpha P^{\frac{k-1}{2k}} \qquad (D.5)$$

The value of the constant $\alpha$ must now be determined. The fluid entering or leaving the tube is by definition extraneous fluid. Fluid from the jet has thus undergone, at most, irreversible changes wrought by one cycle of operation. As will be evident from the yet-to-be constructed wave diagram, the extraneous fluid crosses two major shocks of pressure ratios about two and three. From D.3 it is evident that $\alpha$ is a measure of the irreversibility of the flow which the fluid has passed through. For isentropic flow from the jet, $\alpha = 1$; after passing through the aforementioned shocks, $\alpha = 1.048$. An effective average value of 1.027 is selected and henceforth used for extraneous fluid.

Outflow boundary conditions

The interaction of internal and external flow is now considered, beginning with temporarily steady outflow. The transition to inflow is taken as quasi-steady. In order to show that this is reasonable, convective

acceleration terms may be compared with the unsteady acceleration. In the collision system, fluid from the tube is decelerated from a dimensionless velocity of about one, in a distance of about one diameter. Then

$$(UU_X)_{\theta \text{ fixed}} \quad 1 \cdot \frac{1}{1} = 1$$

At the same position, fluid particles passing a fixed $X$ undergo a change in velocity of one in a time interval $\theta = 20$.

$$(U_\theta)_{X \text{ fixed}} = \frac{1}{20}$$

During the temporarily steady phase, the outflow has proceeded according to internally determined conditions. As the tube is exhausted, however, the outflow impulse must weaken. If the collision system is considered quasi-steady, it is obvious that no outflow whatsoever is possible if the flow has an impulse very much less than the stagnation pressure of the jet. The appropriate pressure limit is that which the jet would exert on a stationary plane face at the tube end, as in the blunt body experiment. It is something less than the stagnation pressure of the jet, denoted by $fP_{oj}$, where $f < 1$. It should be noted that $P_{oj}$

is the stagnation pressure aft of a shock, not the full reservoir pressure.

Then:

i) The outflow remains autonomic so long as its impulse exceeds $fP_{oj}$, a major fraction of the jet stagnation pressure.

As the outflow impulse falls to this value, there is a damming effect exerted against the mouth of the tube by the jet. The outflow impulse cannot subsequently exceed $fP_{oj}$, because lines of constant impulse are about congruent to $C^-$ lines in the pressure-velocity plane, and the time derivative of $C^-$ is positive. Stated more simply, the outflow is weakening. Furthermore, the outflow impulse cannot fall below $fP_{oj}$ by the previous arguments. Then, necessarily:

ii) After falling to the value $fP_{oj}$, the outflow impulse must remain constant.

The value $f = 80\%$ was selected, because it fits the pressure record data. Propositions (i) and (ii), with the state equations, give the required additional equation for U and A for the outflow phase:

$$p + \rho u^2 = fP_{oj}$$

In dimensionless form, with the state equations:

$$P + \frac{k}{\alpha^2} P^{1/k} U^2 = f P_{oj} \qquad (D.6)$$

Since the boundary states will be represented in the P, U plane, equation D.1 is rewritten in terms of pressure by using D.5:

$$U - \frac{2\alpha}{k-1} P^{\frac{k-1}{2k}} = C^- \qquad (D.7)$$

Equations D.6 and D.7 are the required boundary state equations for outflow.

The weakening outflow is initially sonic. It happens that lines of constant impulse and $C^-$ characteristics are congruent at the sonic line (this is demonstrated at the end of the appendix). Referring to figure 21, this requires that a jump take place in the P, U states when the value of $C^-$ is such that this congruence occurs. This of course indicates a shock wave, which is physically identified with the external shock in the outflow, upstream of the collision system. That is, as outflow weakens, this shock moves into the tube.

Inflow boundary conditions

The above considerations apply only until the outflow velocity reaches zero.

As a guide to inflow conditions, the curve for steady isentropic flow downstream of a normal shock is shown on figure 21. It has the equation:

$$C_p T + \frac{u^2}{2} = \text{constant}$$

$$\frac{k}{k-1} \frac{p}{\rho} + \frac{u^2}{2} = \text{constant}$$

In dimensionless form:

$$\frac{1}{k-1} \frac{P}{G} + \frac{U^2}{2} = \text{constant} \qquad (D.8)$$

Using E.3:

$$\frac{1}{\alpha^2(k-1)} P^{\frac{k-1}{k}} + \frac{U^2}{2} = \frac{1}{\alpha^2(k-1)} P_{oj}^{\frac{k-1}{k}} \qquad (D.9)$$

where $\alpha^2$ and $P_{oj}$ are the appropriate values downstream of a normal shock in the jet. For the case considered $\alpha^2 = 1.114$ and $P_{oj} = 5.23$.

Now, since the interface piston is necessarily accelerating into the tube, the inflow has less impulse than for the steady case. The following proposition is evident:

iii) The inflow P, U curve lies to the left of the curve for steady isentropic inflow.

As an additional guide, lines of constant mass flow are drawn in the form of constant fractions e of the full jet mass flow.

$$e = \frac{\rho u}{\rho_a u_a} = \frac{GU}{M_a}$$

$$e = \frac{1}{\alpha^2 M_a} P^{1/k} U \qquad \text{(D.10)}$$

It is recognized that the boundary state curve will assymptotically approach e = 1.

The above conditions, together with the fact that continuity with the outflow curve is required, permit the inflow state curve to be roughly fixed. It is drawn as shown in figure 19.

In the boundary conditions applied, $\alpha$ for outflow was taken as 1.048.

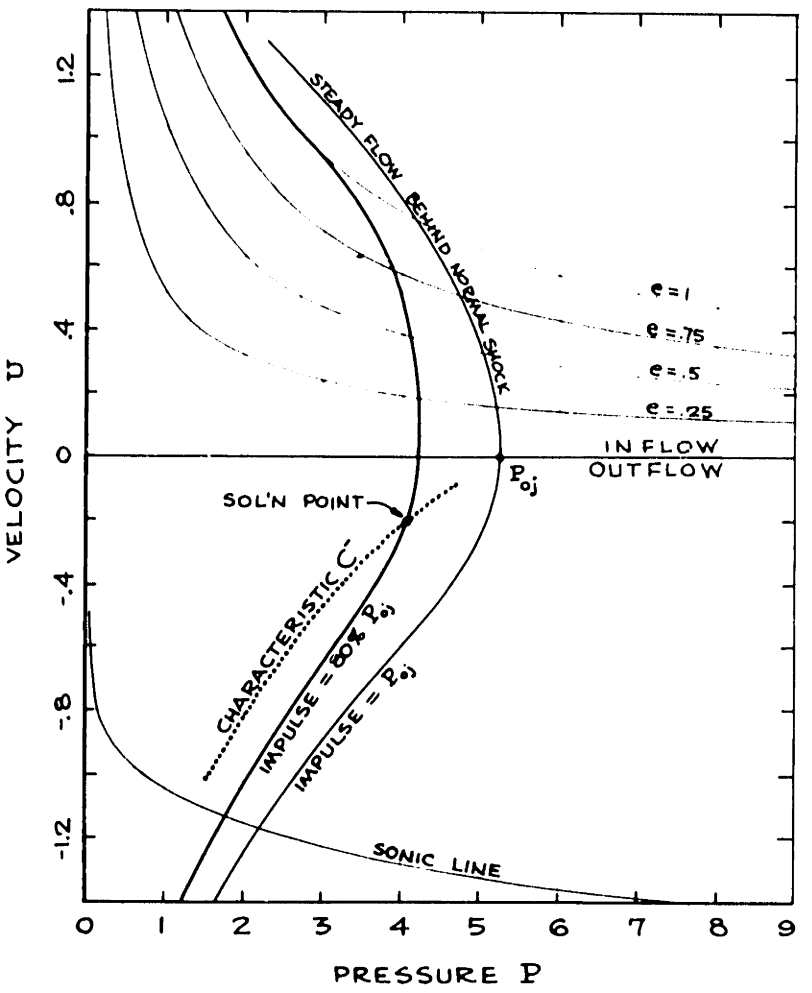


FIG. 19: PRESSURE-VELOCITY BOUNDARY STATES

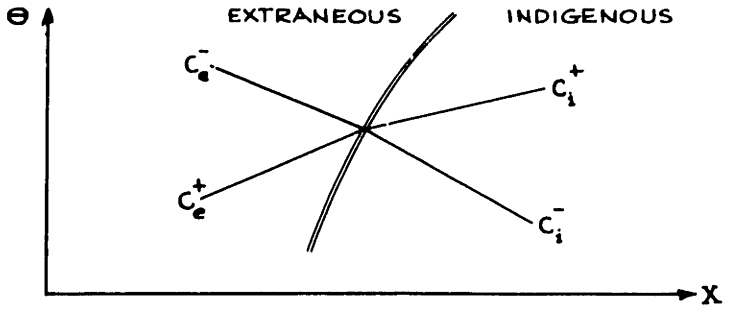


FIG. 20: ENTROPY DISCONTINUITY

Demonstration of the coincidence of constant impulse lines with negative characteristics at the sonic line

The constant impulse line is given by:

$$P + \frac{k}{\alpha^2} P^{1/k} U^2 = \text{constant} \qquad (D.6)$$

The negative characteristic line is

$$U - \frac{2\alpha}{k-1} P^{\frac{k-1}{2k}} = C^- \qquad (D.7)$$

By stipulation the condition is sonic

$$U = -A = -\alpha P^{\frac{k-1}{2k}} \qquad (D.11)$$

Differentiating D.6 with respect to P, and using D.11

$$\frac{dU}{dP} = \frac{\alpha}{k} P^{-\frac{k+1}{2k}} \qquad (D.12)$$

Differentiating D.7 with respect to P

$$\frac{dU}{dP} = \frac{\alpha}{k} P^{-\frac{k+1}{2k}}$$

The slopes of D.6 and D.7 are therefore equal at the sonic line. Similarly, second derivatives are taken, yielding for both curves:

$$\frac{d^2U}{dP^2} = -\frac{k-1}{2k^2}\,\alpha P^{-\frac{3k+1}{2k}} \qquad (D.13)$$

Then D.6 and D.7 are congruent at the sonic line.

## APPENDIX E: HEAT TRANSFER COMPUTATIONS

At a given station, the mean local tempersture is:

$$\bar{T} = \frac{(\Delta B)_e}{B} \bar{T}_e + \frac{(\Delta B)_i}{B} \beta \bar{T}_{ipc} \qquad (E.1)$$

The mean local stagnation temperature is:

$$\bar{T}_o = \frac{(\Delta B)_e}{B} \bar{T}_{oe} + \frac{(\Delta B)_i}{B} \left\{ \beta \bar{T}_{ipc} + \bar{T}_{oipc} - \bar{T}_{ipc} \right\} \qquad (E.2)$$

where $\Delta B$ is the time dwell of indigenous or extraneous fluid and the subscript 'pc' refers to the perfectly cooled model.

Data from the perfectly cooled model

| X | $\frac{(\Delta B)_e}{B}$ | $\frac{(\Delta B)_i}{B}$ | $\bar{T}_e$ | $\bar{T}_{ipc}$ | $\bar{T}_{oe}$ | $\bar{T}_{oicp}$ | $\bar{T}_{oicp}-\bar{T}_{ipc}$ |
|---|---|---|---|---|---|---|---|
| 0 | 1 | 0 | 1.536 | 1.560 | 1.684 | 1.650 | .034 |
| 10 | .681 | .319 | 1.668 | 1.396 | 1.767 | 1.465 | .069 |
| 20 | .512 | .488 | 1.841 | 1.398 | 1.887 | 1.470 | .072 |
| 30 | 0 | 1 | ----- | 1.664 | ----- | 1.687 | .023 |
| 40 | 0 | 1 | ----- | 1.686 | ----- | 1.686 | 0 |

Mean local temperature in a heated tube

Using the above data in E.1 and E.2, there is obtained:

| X | $\bar{T}$ | $\bar{T}_o$ |
|---|---|---|
| 0 | 1.536 | 1.684 |
| 10 | 1.137 + .445$\beta$ | 1.226 + .445$\beta$ |
| 20 | .944 + .682$\beta$ | 1.038 + .682$\beta$ |
| 30 | 1.664$\beta$ | .023 + 1.684$\beta$ |
| 40 | 1.686$\beta$ | 1.686$\beta$ |

where the results are applicable to the perfectly cooled tube for $\beta = 1$.

Heat release

The heat release per cycle is, approximately,

$$Q_{cycle} = m_i(\Delta s)_{cycle}(\beta \bar{\bar{T}}_{ipc})T_a \qquad (E.3)$$

where $\bar{\bar{T}}_{ipc}$ is a space-time average and $T_a$ is dimensional. From the data, $\bar{\bar{T}}_{ipc} = 1.596$.

The indigenous mass is:

$$m_i = \int_0^L \rho a dx = \int_0^L \frac{p}{\beta RT} a dx = \frac{m_{ipc}}{\beta}$$

At full compression $G = 4.14$ and the occupied length is .300 L. Then

$$m_i = \frac{\pi d^2(.300L)4.14\rho_a}{4\beta} = \frac{.310\,\pi\, d^2 L\rho_a}{\beta}$$

The incoming and reflected shocks have Mach Numbers 1.375 and 1.390. This gives stagnation pressure ratios of .9641 and .9606 and an entropy rise

$$(\Delta S)_{cycle} = .0753R$$

Then E.3 becomes

$$\zeta_{cycle} = .310\,\pi\, d^2 L\rho_a\,(.0753R)(1.596)T_a$$

$$\zeta_{cycle} = .0372\,\pi\, d^2 L p_a \qquad \text{(E.4)}$$

Note that, for assumed constant entropy rise per cycle, the heat generation is independent of the tube temperature.

Heat transfer

For periodic operation, the heat transferred from the fluid per cycle is:

$$Q_{cycle} = \pi\, dhBT_a \int_o^L (\overline{T}_o - T_e)dx \qquad (E.5)$$

$$Q_{cycle} = \pi\, d^2hBT_a \int_o^{40} (\overline{T}_o - T_e)dX$$

where h is the overall coefficient of heat transfer. For an environment temperature of 1.691 (slightly less than the reservoir temperature of 1.739), the integral has the value 36.34 $(\beta-1)$. This means that the temperature difference approaches zero as $\beta$ approaches one. Then

$$Q_{cycle} = 36.34\, \pi\, d^2hBT_a(\beta - 1) \qquad (E.6)$$

Equating E.4 and E.6:

$$\beta - 1 = \frac{.032\, \pi\, d^2Lp_a}{36.34\, \pi\, d^2hBT_a}$$

Inserting values for L, B, $p_a$, $T_a$ ($B = 6.8(10)^{-3}$ sec):

$$\frac{Lp_a}{BT_a} = 7.72(10)^3 \frac{BTU}{hr\ ft^{2o}R}$$

then

$$\beta - 1 = \frac{7.90}{h}$$

where $h$ is in $\frac{\text{BTU}}{\text{hr ft}^2\ ^\circ\text{R}}$. Then

$$\beta = 1 + \frac{7.90}{h} \qquad \text{(E.7)}$$

Since $h$ is in the neighborhood of 7.90 for thin walled metal tubes cooled by the airstream, $\beta$ is of order 2. Temperature distributions for various values of $\beta$ are given in figure 14.

## APPENDIX F: CONDITIONS AT AN ENTROPY DISCONTINUITY

For the computation of a wave diagram for an insulated tube, the matching conditions at an entropy discontinuity are needed. The situation is depicted in figure 20. The values of $C_e^+$, $\alpha_e$, $\alpha_i$, and $C_i^-$ are known; the problem is to determine $C_E^-$, $C_I^+$, U, $A_E$ and $A_I$. The matching conditions are:

$$U = U_e = U_i \tag{F.1}$$

$$P = P_e = P_i \tag{F.2}$$

F.2 and D.5 yield:

$$\frac{A_e}{\alpha_e} = \frac{A_i}{\alpha_i}$$

$$\frac{A_e}{A_i} = \frac{\alpha_e}{\alpha_i} \tag{F.3}$$

Then F.3 and the characteristic definition give:

$$C_e^+ = U + \frac{2}{k-1}A_e$$

$$C_i^- = U - \frac{2}{k-1}\frac{\alpha_i}{\alpha_e}A_e$$

These equations and F.3 then give:

$$A_e = \frac{C_e^+ - C_i^-}{\frac{2}{k-1}\left(1 + \frac{\alpha_i}{\alpha_e}\right)} \qquad (F.4)$$

$$A_i = \frac{C_e^+ - C_i^-}{\frac{2}{k-1}\left(1 + \frac{\alpha_e}{\alpha_i}\right)} \qquad (F.5)$$

$$U = \frac{\frac{\alpha_i}{\alpha_e} C_e^+ + C_i^-}{1 + \frac{\alpha_i}{\alpha_e}} \qquad (F.6)$$

The reflected characteristics can then be determined from F.4, F.5 and F.6.

## APPENDIX G: IMPULSE MATCHING BETWEEN JET AND OUTFLOW

For the crude flow model discussed in Section III, the succession of states for extraneous fluid is given by:

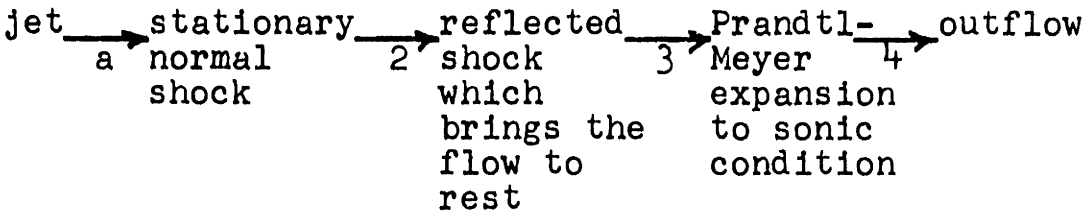


The jet impulse $J_a$ and outflow impulse $J_4$ are to be compared. For one dimensional flows:

$$j = p + \rho u^2 = p(1+kM^2)$$

Define the dimensionless impulse:

$$J = \frac{j}{p_a} = P(1+kM^2) \qquad (G.1)$$

The problem is now worked "backwards" from state 4. Since the outflow is sonic:

$$J_4 = P_4(k+1) \qquad (G.2)$$

For the Prandtl-Meyer expansion:

$$U_4 - \frac{2}{k-1}A_4 = -\frac{2}{k-1}A_3$$

Since $U_4 = -A_4$, there is obtained:

$$\frac{A_4}{A_3} = \frac{2}{k+1} \qquad (G.3)$$

And since the process is isentropic:

$$\frac{P_4}{P_3} = \left(\frac{A_4}{A_3}\right)^{\frac{2k}{k-1}} = \left(\frac{2}{k+1}\right)^{\frac{2k}{k-1}} \qquad (G.4)$$

Then from equations G.2 and G.4

$$J_4 = P_3\left(\frac{2}{k+1}\right)^{\frac{2k}{k-1}}(k+1) \qquad (G.5)$$

The pressure ratio $P_3/P_2$ across the moving shock is given by:

$$\frac{P_3}{P_2} = \frac{2k}{k+1}M_{x2}^2 - \frac{k-1}{k+1} \qquad (G.6)$$

where $M_x$ is the upstream Mach Number, for a coordinate system moving with the shock front. Equation 25.20 of reference 20 gives:

$$M_2 = \frac{2}{k+1}\left(M_{x2} - \frac{1}{M_{x2}}\right) \qquad (G.7)$$

The appropriate root of the quadratic gives:

$$M_{x2}^2 = 2\left(\frac{k+1}{4}\right)^2 M_2^2 + \frac{k+1}{2} M_2 \sqrt{\left(\frac{k+1}{4}\right)^2 M_2^2 + 1} + 1 \qquad (G.8)$$

Across the standing normal shock:

$$J_a = J_2 = P_2(1+kM_2^2)$$

Now, using G.5, G.6, and G.9:

$$\frac{J_4}{J_a} = (k+1)\frac{P_3\left(\frac{2}{k+1}\right)^{\frac{2k}{k-1}}}{P_2(1+kM_2^2)}$$

$$\frac{J_4}{J_a} = \left\{\frac{2k}{k+1} M_{x2}^2 - \frac{k-1}{k+1}\right\}\left\{\frac{(k+1)\left(\frac{2}{k+1}\right)^{\frac{2k}{k-1}}}{1+kM_2^2}\right\}$$

Using G.8 there is obtained:

$$\frac{J_4}{J_a} = \frac{2k\left(\frac{2}{k+1}\right)^{\frac{k+1}{k-1}}}{1+kM_2^2}\left\{\left(\frac{k+1}{4}\right)M_2^2+M_2\sqrt{\left(\frac{k+1}{4}\right)^2M_2^2+1}\quad+\frac{1}{k}\right\} \qquad (G.10)$$

where $M_2$ is obtained from the normal shock condition

$$M_2^2 = \frac{M_a^2+\frac{2}{k-1}}{\frac{2k}{k-1}M_a^2-1} \qquad M_a > 1 \qquad (G.11)$$

or, for subsonic jets,

$$M_2 = M_a \qquad M_a < 1 \qquad (G.12)$$

Then the two equations (G.10 with G.11 or G.12) give the desired relation

$$\frac{J_4}{J_a} = f(M_a)$$

This function is plotted, for various values of k, in figure 21. For all supersonic values of Jet Mach Number,

$$1 > \frac{J_4}{J_a} > 0.9 \qquad (G.13)$$

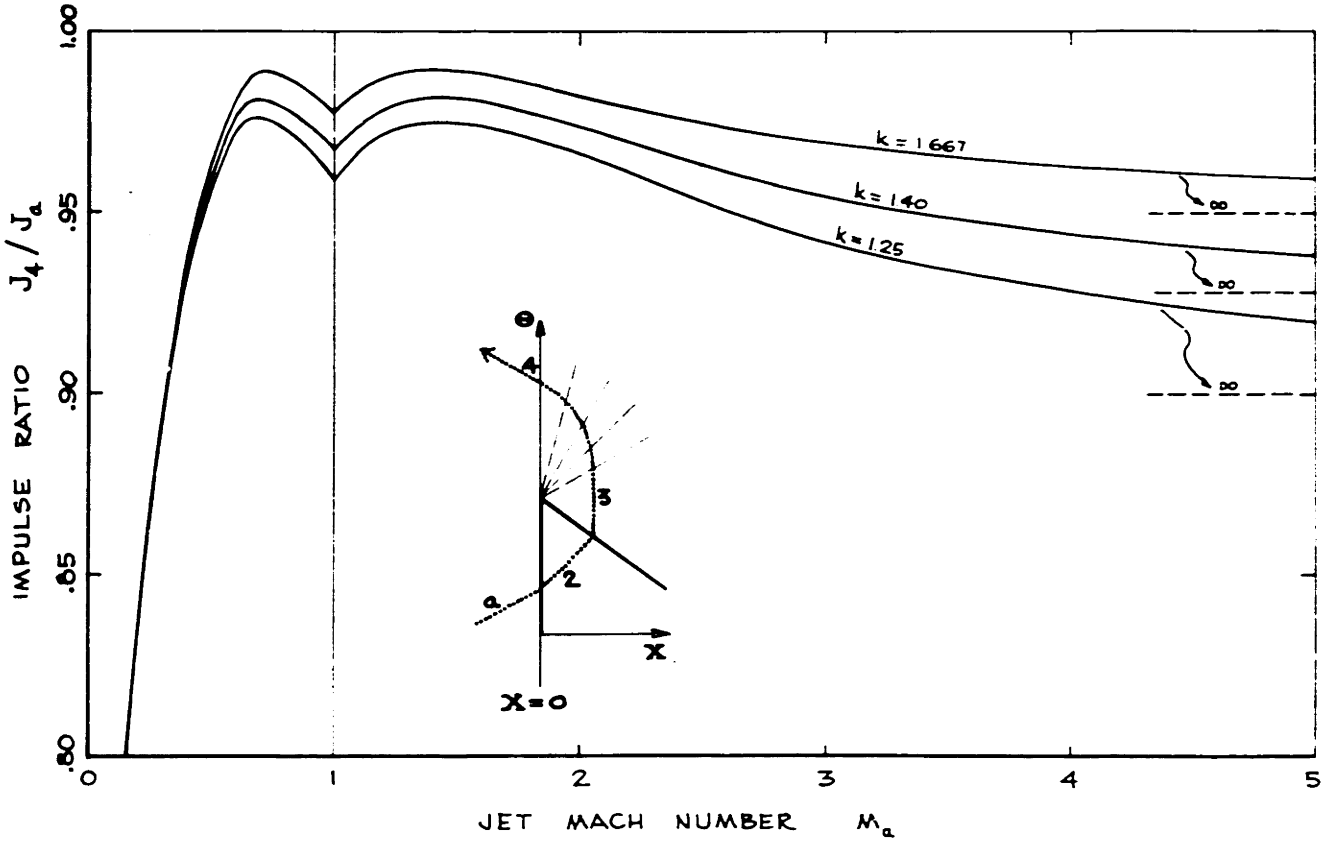


FIG. 21: IMPULSE RATIO vs. JET MACH NUMBER

# APPENDIX H: DATA

## Shadowgraph data

film: Kodak super XX Panchromatic 4 x 5.

developer: Kodak D-76 (11 min.) in tank.

light source: E. G. & G. FX-12.

light setting: high (about 3 microseconds).

distance: source to tube centerline: 50 in.

distance: film to tube centerline: 5.25 in.

## High speed motion picture data

film: Kodak Tri-X Negative, especially for high speed cameras.

developer: Kodak D-76 (12 min.) 20 ft. strip loose in tank.

light source: E. G. & G. FX-21 in 501 strobe.

light setting: .01 microfarad (about 1 microsecond.

distance: source to tube centerline: 48 in.

distance: focal plane to ground glass: 23.3 in.

lens opening: f4.

event delay: .1 sec.

lamp running time: .08 sec.

camera running time: 1.3 sec.

light delay: .96 sec.

light flash rate: 5000 l/sec.

goose voltage: 180 volts.

One high speed film was taken at 10,000 frames per second. This was accomplished by reducing the frame aperture in the high speed camera and running at the speed appropriate to 5000 frames per second. However, the stroboscopic lamp apparently overheated and produced flashes only intermittently.

Ideally cooled tube; characteristic net points

| θ | X | U | A |
|---|---|---|---|
| 00.0 | 40.0 | 0.000 | 1.000 |
| 00.0 | 40.0 | 0.830 | 1.166 |
| 00.0 | 40.0 | 0.000 | 1.336 |
| 05.7 | 40.0 | 0.000 | 1.364 |
| 13.6 | 00.0 | 0.740 | 1.268 |
| 23.1 | 20.2 | 0.940 | 1.288 |
| 37.1 | 40.0 | 0.000 | 1.416 |
| 46.6 | 00.0 | 0.870 | 1.245 |
| 46.6 | 00.0 | 0.090 | 1.401 |
| 75.1 | 40.0 | 0.000 | 1.419 |
| 76.7 | 37.0 | -0.147 | 1.390 |
| 78.2 | 35.2 | -0.247 | 1.370 |
| 78.9 | 40.0 | 0.000 | 1.360 |
| 79.7 | 33.0 | -0.347 | 1.350 |
| 80.5 | 37.9 | -0.100 | 1.340 |
| 81.1 | 30.4 | -0.447 | 1.330 |
| 82.1 | 35.5 | -0.200 | 1.320 |
| 82.3 | 40.0 | 0.000 | 1.320 |
| 82.7 | 27.4 | -0.547 | 1.310 |
| 83.9 | 32.8 | -0.300 | 1.300 |
| 84.0 | 37.6 | -0.100 | 1.300 |
| 85.8 | 29.8 | -0.400 | 1.280 |
| 85.9 | 34.9 | -0.200 | 1.280 |
| 85.9 | 40.0 | 0.000 | 1.280 |
| 86.5 | 20.6 | -0.747 | 1.270 |
| 87.9 | 32.0 | -0.300 | 1.260 |
| 87.9 | 37.2 | -0.100 | 1.260 |
| 89.8 | 22.6 | -0.600 | 1.240 |
| 90.2 | 34.2 | -0.200 | 1.240 |
| 90.2 | 40.0 | 0.000 | 1.240 |
| 90.3 | 12.3 | -0.947 | 1.230 |
| 92.5 | 07.5 | -1.047 | 1.210 |
| 92.5 | 24.5 | -0.500 | 1.220 |
| 92.6 | 36.8 | -0.100 | 1.220 |
| 93.6 | 04.7 | -1.097 | 1.200 |

| θ | X | U | A |
|---|---|---|---|
| 94.5 | 13.6 | -0.800 | 1.200 |
| 94.8 | 02.0 | -1.147 | 1.190 |
| 95.3 | 26.5 | -0.400 | 1.200 |
| 95.3 | 40.0 | 0.000 | 1.200 |
| 95.5 | 00.0 | -1.182 | 1.182 |
| 97.0 | 08.4 | -0.900 | 1.180 |
| 97.6 | 15.2 | -0.700 | 1.180 |
| 98.2 | 29.2 | -0.300 | 1.180 |
| 98.4 | 05.5 | -0.950 | 1.170 |
| 99.8 | 02.5 | -1.000 | 1.100 |
| 100.6 | 00.5 | -1.034 | 1.153 |
| 100.6 | 09.5 | -0.800 | 1.160 |
| 100.9 | 00.0 | -0.750 | 1.210 |
| 101.0 | 16.9 | -0.600 | 1.160 |
| 101.5 | 32.2 | -0.200 | 1.160 |
| 102.1 | 06.5 | -0.850 | 1.150 |
| 103.7 | 03.4 | -0.900 | 1.140 |
| 104.4 | 11.2 | -0.700 | 1.140 |
| 104.6 | 19.2 | -0.500 | 1.140 |
| 105.5 | 00.0 | -0.207 | 1.279 |
| 106.0 | 07.8 | -0.750 | 1.130 |
| 107.9 | 04.4 | -0.800 | 1.120 |
| 108.2 | 13.1 | -0.600 | 1.120 |
| 108.7 | 21.8 | -0.400 | 1.120 |
| 109.0 | 40.0 | 0.000 | 1.120 |
| 110.2 | 09.5 | -0.650 | 1.110 |
| 110.9 | 00.0 | 0.028 | 1.286 |
| 112.6 | 15.6 | -0.500 | 1.100 |
| 113.9 | 04.2 | 0.128 | 1.266 |
| 114.9 | 11.9 | -0.550 | 1.090 |
| 117.1 | 08.9 | 0.228 | 1.246 |
| 117.6 | 00.0 | 0.230 | 1.286 |
| 117.8 | 29.4 | -0.200 | 1.080 |
| 121.0 | 05.2 | 0.330 | 1.266 |
| 123.0 | 22.5 | -0.300 | 1.060 |
| 126.7 | 00.0 | 0.410 | 1.282 |
| 128.3 | 17.4 | 0.530 | 1.226 |
| 134.2 | 13.5 | 0.610 | 1.242 |
| 157.3 | 00.0 | 0.740 | 1.268 |

Insulated tube: characteristic net points

| θ | X | U | A |
|---|---|---|---|
| 00.7 | 11.6 | 0.879 | 1.216 |
| 00.7 | 11.6 | 0.879 | 2.432 |
| 03.1 | 33.7 | 1.206 | 2.381 |
| 03.5 | 20.7 | 1.021 | 2.404 |
| 05.6 | 40.0 | 0.000 | 2.622 |
| 06.3 | 16.7 | 0.992 | 1.199 |
| 06.3 | 16.7 | 0.992 | 2.398 |
| 08.0 | 34.0 | -0.035 | 2.615 |
| 10.1 | 40.0 | 0.000 | 2.608 |
| 10.1 | 20.5 | 1.066 | 1.188 |
| 10.1 | 20.5 | 1.066 | 2.376 |
| 10.1 | 20.5 | -0.107 | 2.610 |
| 10.1 | 20.5 | 0.284 | 2.688 |
| 10.1 | 20.5 | 0.284 | 1.344 |
| 10.1 | 28.2 | -0.064 | 2.610 |
| 12.3 | 34.1 | -0.029 | 2.603 |
| 14.6 | 40.0 | 0.000 | 2.597 |
| 15.5 | 07.1 | 0.949 | 1.230 |
| 17.0 | 10.7 | 1.000 | 1.220 |
| 17.2 | 22.5 | 0.353 | 2.680 |
| 17.2 | 22.5 | 0.353 | 1.340 |
| 18.7 | 14.4 | 1.048 | 1.210 |
| 19.2 | 29.0 | 0.382 | 2.673 |
| 21.0 | 18.7 | 0.378 | 1.344 |
| 21.1 | 34.8 | 0.018 | 2.746 |
| 21.3 | 24.1 | 0.391 | 2.674 |
| 21.3 | 24.1 | 0.391 | 1.337 |
| 23.0 | 40.0 | 0.000 | 2.750 |
| 23.1 | 29.5 | 0.027 | 2.748 |
| 23.2 | 22.4 | 0.402 | 1.340 |
| 24.8 | 25.0 | 0.163 | 2.774 |
| 24.8 | 25.0 | 0.163 | 1.387 |
| 25.0 | 34.5 | 0.009 | 2.751 |
| 26.6 | 30.5 | 0.145 | 2.779 |
| 27.0 | 40.0 | 0.000 | 2.753 |

| θ | X | U | A |
|---|---|---|---|
| 28.4 | 25.6 | 0.149 | 2.780 |
| 28.4 | 25.6 | 0.149 | 1.390 |
| 28.5 | 36.1 | 0.136 | 2.780 |
| 29.0 | 03.3 | 0.944 | 1.229 |
| 29.0 | 40.0 | 0.000 | 2.808 |
| 30.3 | 31.2 | 0.140 | 2.781 |
| 31.0 | 07.5 | 0.995 | 1.219 |
| 31.6 | 08.5 | 0.372 | 1.344 |
| 31.6 | 35.0 | 0.004 | 2.808 |
| 32.3 | 26.1 | 0.142 | 2.782 |
| 32.3 | 26.1 | 0.142 | 1.391 |
| 33.5 | 29.9 | 0.006 | 2.809 |
| 33.8 | 12.4 | 0.397 | 1.339 |
| 34.3 | 13.2 | 0.158 | 1.383 |
| 34.8 | 06.3 | 0.050 | 2.818 |
| 34.8 | 06.3 | 0.050 | 1.409 |
| 36.1 | 16.0 | 0.145 | 1.389 |
| 37.1 | 40.0 | 0.000 | 2.810 |
| 37.9 | 18.6 | 0.139 | 1.390 |
| 38.4 | 36.7 | 0.044 | 2.819 |
| 39.1 | 20.5 | 0.048 | 1.408 |
| 39.5 | 00.0 | 0.000 | 2.828 |
| 39.9 | 00.0 | 0.940 | 1.228 |
| 41.8 | 26.7 | 0.044 | 1.409 |
| 41.8 | 26.7 | 0.044 | 2.818 |
| 43.1 | 30.0 | 0.000 | 2.828 |
| 43.6 | 06.6 | 0.141 | 1.388 |
| 44.1 | 00.0 | 0.384 | 1.339 |
| 44.2 | 26.8 | 0.014 | 2.830 |
| 44.2 | 26.8 | 0.014 | 1.415 |
| 45.4 | 09.4 | 0.135 | 1.389 |
| 46.3 | 10.6 | 0.044 | 1.408 |
| 46.6 | 40.0 | 0.000 | 2.828 |
| 47.6 | 36.9 | 0.014 | 2.830 |
| 48.7 | 40.0 | 0.000 | 2.833 |
| 50.0 | 15.7 | 0.040 | 1.408 |
| 51.0 | 17.2 | 0.010 | 1.414 |
| 51.2 | 26.9 | 0.011 | 2.830 |
| 51.2 | 26.9 | 0.011 | 1.415 |
| 53.3 | 27.0 | 0.001 | 2.834 |

| θ | X | U | A |
|---|---|---|---|
| 53.3 | 27.0 | 0.001 | 1.417 |
| 54.5 | 22.2 | 0.009 | 1.415 |
| 58.0 | 40.0 | 0.000 | 2.834 |
| 62.4 | 26.9 | -0.004 | 2.832 |
| 62.4 | 26.9 | -0.004 | 1.416 |
| 64.0 | 24.6 | -0.188 | 1.380 |
| 65.5 | 26.5 | -0.249 | 2.784 |
| 65.5 | 26.5 | -0.249 | 1.392 |
| 65.8 | 21.6 | -0.388 | 1.340 |
| 67.0 | 40.0 | 0.000 | 2.832 |
| 67.4 | 23.2 | -0.449 | 1.352 |
| 67.8 | 18.0 | -0.588 | 1.300 |
| 68.9 | 34.7 | -0.246 | 2.783 |
| 69.6 | 19.2 | -0.649 | 1.312 |
| 69.6 | 25.0 | -0.514 | 2.730 |
| 69.6 | 25.0 | -0.514 | 1.365 |
| 70.0 | 13.6 | -0.788 | 1.260 |
| 70.8 | 40.0 | 0.000 | 2.734 |
| 70.9 | 28.3 | -0.512 | 2.730 |
| 71.7 | 20.6 | -0.714 | 1.325 |
| 72.0 | 14.5 | -0.849 | 1.272 |
| 72.7 | 08.1 | -0.988 | 1.220 |
| 73.1 | 33.4 | -0.266 | 2.680 |
| 74.1 | 22.0 | -0.740 | 2.660 |
| 74.1 | 22.0 | -0.740 | 1.330 |
| 74.2 | 15.4 | -0.914 | 1.285 |
| 74.7 | 08.5 | -1.049 | 1.232 |
| 75.6 | 01.2 | -1.188 | 1.180 |
| 75.7 | 40.0 | 0.000 | 2.627 |
| 75.7 | 25.4 | -0.554 | 2.623 |
| 76.8 | 16.2 | -0.940 | 1.290 |
| 77.1 | 08.9 | -1.114 | 1.245 |
| 77.8 | 01.1 | -1.249 | 1.192 |
| 78.7 | 31.9 | -0.288 | 2.570 |
| 79.8 | 09.2 | -1.140 | 1.250 |
| 79.9 | 17.5 | -0.839 | 2.540 |
| 79.9 | 17.5 | -0.839 | 1.270 |
| 80.4 | 01.0 | -1.314 | 1.205 |
| 82.1 | 40.0 | 0.000 | 2.512 |
| 82.2 | 21.7 | -0.638 | 2.499 |

| Θ | X | U | A |
|---|---|---|---|
| 83.3 | 00.6 | -1.340 | 1.210 |
| 83.5 | 09.8 | -1.039 | 1.230 |
| 86.2 | 29.5 | -0.351 | 2.442 |
| 87.4 | 00.3 | -1.239 | 1.190 |
| 87.6 | 10.8 | -0.915 | 2.410 |
| 87.6 | 10.8 | -0.915 | 1.205 |
| 90.8 | 40.0 | 0.000 | 2.372 |
| 90.9 | 15.9 | -0.713 | 2.369 |
| 92.5 | 00.4 | -1.115 | 1.165 |
| 94.3 | 04.7 | -0.942 | 2.324 |
| 94.3 | 04.7 | -0.942 | 1.162 |
| 96.2 | 00.6 | -1.020 | 1.146 |
| 96.5 | 25.8 | -0.362 | 2.299 |
| 96.6 | 00.0 | -0.500 | 1.250 |
| 97.7 | 03.4 | -0.926 | 2.285 |
| 99.1 | 00.0 | 0.120 | 1.286 |
| 100.1 | 00.8 | 0.286 | 1.253 |
| 100.1 | 00.8 | 0.286 | 2.506 |
| 100.6 | 14.4 | -0.591 | 2.253 |
| 101.2 | 00.0 | 0.440 | 1.283 |
| 102.2 | 09.9 | -0.679 | 2.236 |
| 102.6 | 08.7 | 0.478 | 2.467 |
| 102.9 | 02.9 | 0.578 | 1.256 |
| 102.9 | 02.9 | 0.578 | 2.512 |
| 103.1 | 40.0 | 0.000 | 2.227 |
| 104.0 | 06.2 | 0.640 | 2.499 |
| 104.5 | 21.3 | -0.412 | 2.218 |
| 107.0 | 15.9 | 0.818 | 2.464 |
| 107.2 | 00.0 | 0.660 | 1.272 |
| 108.2 | 28.2 | -0.229 | 2.181 |
| 109.7 | 04.9 | 0.767 | 1.251 |
| 109.8 | 25.3 | 1.001 | 2.427 |
| 112.1 | 10.0 | 0.873 | 1.229 |
| 112.1 | 10.0 | 0.873 | 2.459 |
| 114.3 | 40.0 | 1.232 | 2.322 |
| 114.5 | 29.5 | 1.126 | 2.405 |
| 114.6 | 18.5 | 1.017 | 2.430 |

## APPENDIX I: DYADIC JET EQUATIONS

The equations are derived using cylindrical coordinates for a wedge-shaped control volume of central angle $d\emptyset$ and length $dx$, with the outer surface corresponding to the instantaneous jet boundary. Diameter of the jet is $d^*$; dimensionless jet diameter $D = d^*/d$. An average density $\rho$ is used, together with an average axial velocity $u$. That is,

$$\rho = \rho(x,t)$$
$$u = u(x,t)$$

### Boundary conditions

Pressure and radial velocity $v$ are taken to vary with radius. Continuity requires that at the centerline

$$v(o,x,t) = 0 \qquad \text{(I.1)}$$

The momentum theorem gives

$$p_r(o,x,t) = 0 \qquad \text{(I.2)}$$

The approximate condition at $p$ at the atmospheric

boundary is

$$p(\frac{d^*}{2},x,t) = p_a \qquad (I.3)$$

Pressure and velocity distributions

The simplest distributions $p(r)$ and $v(r)$, satisfying the above boundary conditions, are assumed:

$$v = v_1 \frac{r}{d^*/2} \qquad (I.4)$$

$$p = p_c - (p_c - p_a)(\frac{r}{d^*/2})^2 \qquad (I.5)$$

where $p_c$ is the centerline pressure.

The following dimensionless forms will also be used:

$N = \frac{r}{d^*/2}$ dimensionless radius

$V = \frac{v_1}{a_a}$ dimensionless radial boundary velocity

The boundary equation

This states that the convective derivation of the boundary radius is equal to the radial velocity at the

boundary:

$$\frac{\partial}{\partial t}\left(\frac{d^*}{2}\right) + u\frac{\partial}{\partial x}\left(\frac{d^*}{2}\right) = v_1$$

In dimensionless form:

$$D_\theta + UD_X = 2V \qquad \text{(I.6)}$$

Continuity

The net inflow is balanced against the rate of mass increase:

$$\frac{\partial}{\partial x}\int_0^{d^*/2} \rho ur \, d\phi dx dr + \frac{\partial}{\partial t}\int_0^{d^*/2} \rho ur \, d\phi dx dr = 0$$

or in dimensionless form

$$\frac{\partial}{\partial X} GUD^2 \int_0^1 N dN + \frac{\partial}{\partial \theta} GD^2 \int_0^1 N dN = 0$$

$$\frac{\partial}{\partial X}(GUD^2) + \frac{\partial}{\partial \theta}(GD^2) = 0$$

which could have been written directly. Expanded, and

using the boundary equation D.6:

$$G_\theta + GU_X + UG_X + 4\frac{GV}{D} = 0 \qquad (I.7)$$

which is the usual dimensionless continuity equation with the addition of a radial 'leakage' term.

Axial momentum

The momentum theorem for a control volume gives:

$$\frac{\partial}{\partial x}\int_0^{d^*/2}(p+\rho u^2)\, r\,d\phi\,dx\,dr - p_a\,\frac{d^*}{2}\,\frac{\partial(d^*/2)}{\partial x}\,dx\,d\phi + \frac{\partial}{\partial t}\int_0^{d^*/2}\rho u r\,d\phi\,dx\,dr = 0$$

$$\frac{\partial}{\partial X}D^2\int_0^1\left(\frac{p}{p_a}+kGU^2\right)N\,dN - DD_X + \frac{\partial}{\partial\theta}kD^2\int_0^1 GUN\,dN = 0$$

The mean dimensionless pressure $P$ is defined as that

which gives equal force over the jet cross section, i.e. -

$$\pi (1)^2 P = \int_0^1 2\pi \frac{p}{p_a} N dN$$

$$P = 2 \int_0^1 \frac{p}{p_a} N dN = P(X,\theta) \qquad (I.8)$$

Then applying this to the momentum equation and integrating

$$\frac{\partial}{\partial X} D^2 (P + kGU^2) - 2DD_X + \frac{\partial}{\partial \theta} kD^2 GU = 0$$

After expanding and using the boundary and continuity equations:

$$U_\theta + UU_X + \frac{P_X}{kG} + \frac{2}{k} \frac{P-1}{GD} D_X = 0 \qquad (I.9)$$

which is the conventional one-dimensional momentum equation, with the addition of a term accounting for axial boundary forces.

Radial momentum

Applying the momentum theorem for radial flux gives:

$$\int_0^{d^*/2} pd\phi dxdr - p_a \frac{d^*}{2} d\phi dx = \frac{\partial}{\partial x} \int_0^{d^*/2} \rho uvr \, d\phi dxdr + \frac{\partial}{\partial t} \int_0^{d^*/2} \rho vr \, d\phi dxdr$$

In dimensionless form:

$$D \int_0^1 \frac{p}{p_a} dN - D = \frac{\partial}{\partial X} \frac{k}{2} D^2 GUV \int_0^1 N^2 dN + \frac{\partial}{\partial \theta} \frac{k}{2} D^2 GV \int_0^1 N^2 dN$$

Using I.5:

$$\int_0^1 \frac{p}{p_a} dN = \frac{p_c}{p_a} - \frac{1}{3} \left(\frac{p_c}{p_a} - 1\right)$$

$$\int_0^1 \frac{p}{p_a} NdN = \frac{1}{2} \frac{p_c}{p_a} - \frac{1}{4} \left(\frac{p_c}{p_a} - 1\right) = \frac{P}{2}$$

then

$$\int_0^1 \frac{p}{p_a}\, dN = \frac{4P-1}{3} \qquad (I.10)$$

Using this, the momentum equation becomes:

$$\frac{\partial}{\partial \theta} kD^2GV + \frac{\partial}{\partial X} kD^2GUV + 4D(1-P) = 0$$

Expanding, using the continuity and boundary equations:

$$V_\theta + UV_X + \frac{4}{k}\frac{1-P}{DG} = 0 \qquad (I.11)$$

Characteristic form of the equations

For the unknowns U, V, P and D, the following equations have been derived:

$$D_\theta + UD_X = 2V \qquad (I.6)$$

$$G_\theta + GU_X + UG_X + 4\frac{GV}{D} = 0 \qquad (I.7)$$

$$U_\theta + UU_X + \frac{P_X}{kG} + \frac{2}{k}\frac{P-1}{DG} D_X = 0 \qquad (I.9)$$

$$V_\theta + UV_X + \frac{4}{k}\frac{1-P}{DG} = 0 \qquad \text{(I.11)}$$

For isentropic flow,

$$P = G^k \qquad \text{(I.12)}$$

Also

$$P/G = G^{k-1} = P^{-\frac{k-1}{k}} = A^2$$

Using the above equation, after taking logarithmic derivatives:

$$\frac{P_{X,\theta}}{P} = \frac{2k}{k-1}\frac{A_{X,\theta}}{A} \qquad \text{(I.13)}$$

$$\frac{G_{X,\theta}}{G} = \frac{2}{k-1}\frac{A_{X,\theta}}{A} \qquad \text{(I.14)}$$

Using I.13 and I.14, equations D.8 and D.10 become:

$$\frac{2}{k-1}A_\theta + \frac{2}{k-1}UA_X + AU_X = -\frac{4V}{D} \qquad \text{(I.15)}$$

$$U_\theta + \frac{2}{k-1}AA_X + UU_X = -\frac{2A^2}{k}(1-A^{\frac{2k}{k-1}})\frac{D_X}{D} \qquad \text{(I.16)}$$

Adding and subtracting I.15 and I.16, and rewriting the radial momentum and boundary equations, the complete dyadic equations become

$$\left\{\frac{\partial}{\partial\theta} + (U+A)\frac{\partial}{\partial X}\right\}\left\{U + \frac{2}{k-1}A\right\} = -\frac{4V}{D} - \frac{2A^2}{k}(1-A^{\frac{-2k}{k-1}})\frac{D_X}{D} \qquad (I.17)$$

$$\left\{\frac{\partial}{\partial\theta} + (U-A)\frac{\partial}{\partial X}\right\}\left\{U - \frac{2}{k-1}A\right\} = +\frac{4V}{D} - \frac{2A^2}{k}(1-A^{\frac{-2k}{k-1}})\frac{D_X}{D} \qquad (I.18)$$

$$V_\theta + UV_X = \frac{4A^2}{kD}(1-A^{\frac{-2k}{k-1}}) \qquad (I.19)$$

$$D_\theta + UD_X = 2V \qquad (I.6)$$

which is the required characteristic set for the unknowns, U, A, V, D. For true one-dimensional flows, V and $D_{X,\theta}$ are identically zero, and the above equations reduce to 5.1 and 5.2.

Steady flows

To test the suitability of the dyadic equations, two trial solutions have been worked out. For steady flows, the equations become

$$U_X = \frac{4V}{D(U^2-A^2)} \left\{ A - \frac{A^2}{k}\left(1-A^{\frac{-2k}{k-1}}\right) \right\} \qquad (I.20)$$

$$A_X = \frac{4V}{5D(U^2-A^2)} \left\{ -U + \frac{A^3}{kU}\left(1-A^{\frac{-2k}{k-1}}\right) \right\} \qquad (I.21)$$

$$V_X = \frac{4A^2}{kDU}\left(1-A^{\frac{-2k}{k-1}}\right) \qquad (I.22)$$

$$D_X = \frac{2V}{U} \qquad (I.23)$$

In equation I.20, $U_X$ vanishes for $A = 1.491$. ($U \neq A$, $k = 1.400$).

Solutions are presented in figure 22.

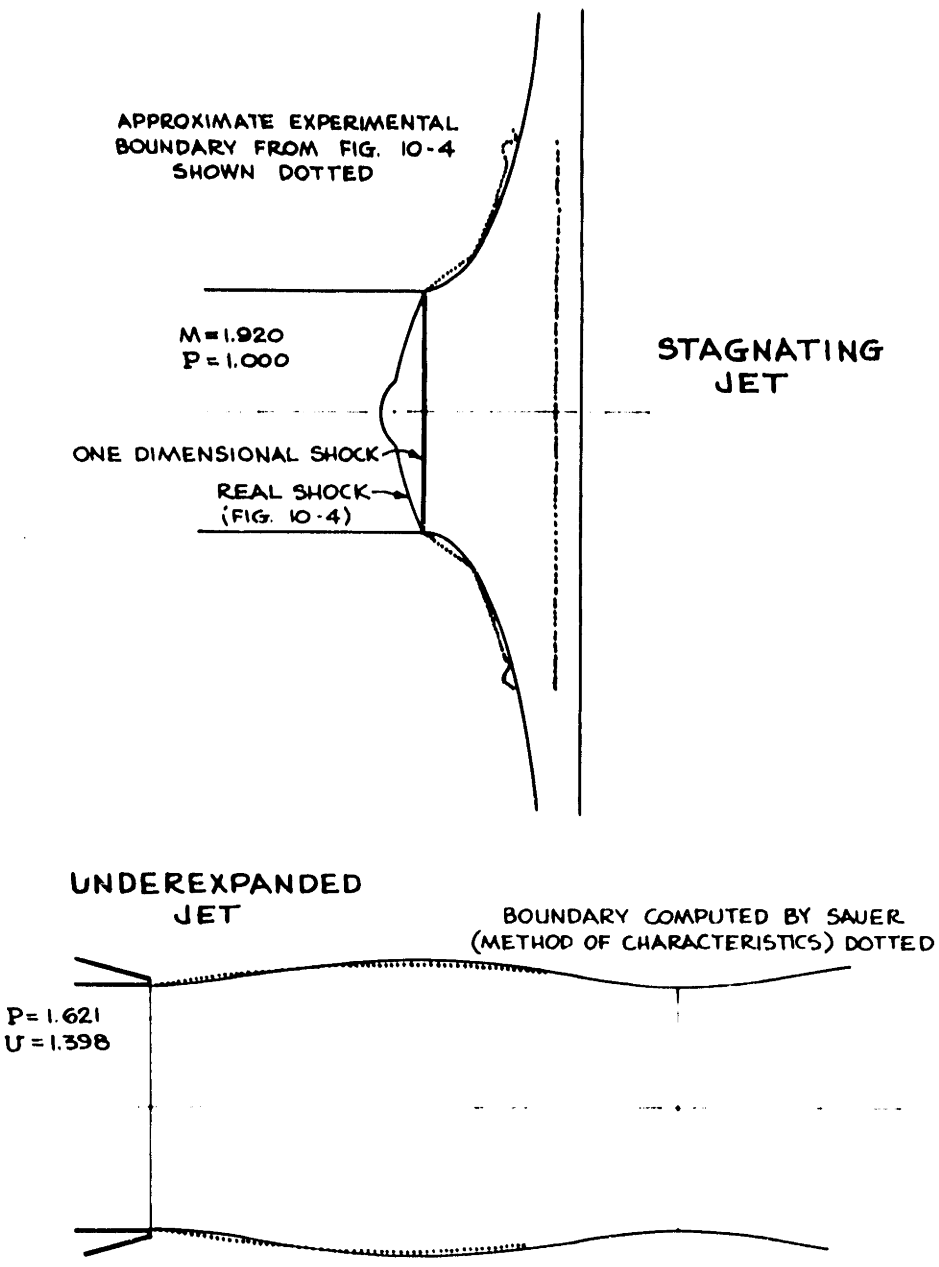


FIG 22: COMPUTED SOLUTIONS - DYADIC EQUATIONS

## Stagnating jet solution

A straight supersonic jet, Mach Number 1.92, is incident on a plane wall. By taking a normal shock at $X = 0$, and applying one-dimensional shock conditions, the variables at $X = 0^+$ are obtained. U, A, and V are normalized with respect to downstream sound speed at $P = 1$. The solution is computed using equations I.20 through I.23 and compared with the jet boundary seen in the external flow shadowgraph, figure 10-4.

$$P_o = 4.134$$

$$k = 1.40$$

$$\Delta X = .001$$

| X | U | A | V | D | $D^2UA^5$ |
|---|---|---|---|---|---|
| $0^+$ | .7248 | 1.2248 | 0 | 1.0000 | 2.00 |
| .050 | .7155 | 1.2218 | .22327 | 1.0152 | 2.01 |
| .100 | .6881 | 1.2132 | .44113 | 1.0623 | 2.04 |
| .150 | .6445 | 1.1993 | .64856 | 1.1439 | 2.09 |
| .200 | .5875 | 1.1812 | .84159 | 1.2647 | 2.16 |
| .250 | .5203 | 1.1597 | 1.01740 | 1.4326 | 2.24 |
| .300 | .4461 | 1.1360 | 1.17436 | 1.6597 | 2.33 |
| .350 | .3680 | 1.1113 | 1.31178 | 1.9659 | 2.41 |
| .400 | .2892 | 1.0867 | 1.42960 | 2.3849 | 2.49 |
| .450 | .2129 | 1.0632 | 1.52812 | 2.9786 | 2.57 |
| .500 | .1425 | 1.0418 | 1.60773 | 3.8741 | 2.63 |
| .550 | .0819 | 1.0238 | 1.66879 | 5.3793 | 2.67 |
| .600 | .0353 | 1.0102 | 1.71151 | 8.4866 | 2.68 |
| .650 | .0069 | 1.0019 | 1.73585 | 19.2536 | 2.59 |

## Underexpanded jet solution

A supersonic flow issues from a straight nozzle with slight overpressure, P(0) = 1.621. The solution is computed by equations I.20 through I.23 and compared with one given by Sauer.[23]

$P(0) = 1.621$

$k = 1.40$

$\Delta X = .001$

| X | U | A | V | D | $D^2UA^5$ |
|---|---|---|---|---|---|
| 0 | 1.3984 | 1.0716 | 0 | 1.0000 | 1.98 |
| 0.10 | 1.4144 | 1.0666 | .0876 | 1.0062 | 1.98 |
| 0.20 | 1.4564 | 1.0535 | .1624 | 1.0238 | 1.98 |
| 0.30 | 1.5122 | 1.0357 | .2163 | 1.0495 | 1.99 |
| 0.40 | 1.5719 | 1.0164 | .2467 | 1.0798 | 1.99 |
| 0.50 | 1.6300 | .9976 | .2541 | 1.1113 | 1.99 |
| 0.60 | 1.6825 | .9805 | .2426 | 1.1416 | 1.99 |
| 0.70 | 1.7277 | .9660 | .2138 | 1.1685 | 1.99 |
| 0.80 | 1.7641 | .9545 | .1717 | 1.1907 | 1.98 |
| 0.90 | 1.7908 | .9461 | .1197 | 1.2072 | 1.98 |
| 1.00 | 1.8069 | .9411 | .0610 | 1.2174 | 1.98 |
| 1.10 | 1.8123 | .9394 | -.0008 | 1.2207 | 1.98 |
| 1.20 | 1.8067 | .9412 | -.0627 | 1.2172 | 1.98 |
| 1.30 | 1.7904 | .9463 | -.1213 | 1.2070 | 1.98 |
| 1.40 | 1.7636 | .9547 | -.1733 | 1.1904 | 1.98 |
| 1.50 | 1.7269 | .9663 | -.2153 | 1.1680 | 1.99 |
| 1.60 | 1.6814 | .9809 | -.2439 | 1.1409 | 1.99 |
| 1.70 | 1.6285 | .9980 | -.2557 | 1.1105 | 1.99 |
| 1.80 | 1.5702 | 1.0169 | -.2475 | 1.0789 | 1.99 |
| 1.90 | 1.5101 | 1.0364 | -.2165 | 1.0485 | 1.99 |
| 2.00 | 1.4540 | 1.0542 | -.1620 | 1.0226 | 1.98 |
| 2.10 | 1.4117 | 1.0674 | -.0863 | 1.0050 | 1.98 |
| 2.20 | 1.3959 | 1.0723 | .0024 | .9989 | 1.98 |
| 2.30 | 1.4135 | 1.0671 | .0906 | 1.0054 | 1.98 |
| 2.40 | 1.4561 | 1.0532 | .1663 | 1.0237 | 1.98 |
| 2.50 | 1.5131 | 1.0354 | .2196 | 1.0499 | 1.99 |
| 2.60 | 1.5735 | 1.0159 | .2496 | 1.0805 | 1.99 |

Small perturbation equations

Consider a steady flow, for which the solution of the dyadic equation gives

$$U = U_o(X)$$
$$A = A_o(X)$$
$$V = V_o(X)$$
$$D = D_o(X)$$

If small unsteady perturbations of this flow take place

$$\begin{aligned} U &= U_o(X) + u(X,\theta) \\ A &= A_o(X) + a(X,\theta) \\ V &= V_o(X) + v(X,\theta) \\ D &= D_o(X) + d(X,\theta) \end{aligned} \qquad (I.24)$$

where the small letters u, a, v, d now represent dimensionless quantities. It is assumed that the perturbations are small. For example

$$U_o \gg u$$

The variables I.24 are substituted into the dyadic equations. The equations obtained correspond to

the form

$$(M+m)_\theta + (M+m)(M+m)_X = F + f \qquad (I.25)$$

where the small letters again represent perturbation quantities. Expanding the left side, and subtracting out the steady solution

$$m_\theta + Mm_X + m(M+m)_X = f$$

The last term on the left hand side is dropped, because $m$ is taken as small while its derivatives are not.

$$m_\theta + Mm_X = f \qquad (I.26)$$

The perturbation quantities corresponding to $f$ are obtained from the binomial theorem. For example, the term $4V/D$ appearing in I.17 and I.18 is

$$4\frac{V}{D} = 4\frac{V_o+v}{D_o+d} = 4\frac{V_o}{D_o}\frac{1+\frac{v}{V_o}}{1+\frac{d}{D_o}}$$

Since $\frac{v}{V_o}$ and $\frac{d}{D_o}$ are small, this is approximated by

$$4\frac{V}{D} = 4\frac{V_o}{D_o}\left(1 + \frac{v}{V_o}\right)\left(1 - \frac{d}{D_o}\right)$$

$$4\frac{V}{D} = 4\frac{V_o}{D_o}\left(1 + \frac{v}{V_o} - \frac{d}{D_o}\right)$$

There is finally obtained the perturbation dyadic equations:

$$\left(u + \frac{2}{k-1}a\right)_\theta + (U_o + A_o)\left(u + \frac{2}{k-1}a\right)_X = -\frac{4v}{D_o} - g \qquad (I.27)$$

$$\left(u - \frac{2}{k-1}a\right)_X + (U_o - A_o)\left(u - \frac{2}{k-1}a\right)_X = +\frac{4v}{D_o} - g \qquad (I.28)$$

$$v_\theta + U_o v_X = h \qquad (I.29)$$

$$d_\theta + U_o d_X = 2v \qquad (I.30)$$

where

$$g = \frac{2}{k}\frac{A_o^2}{D_o}\left(1 - A_o^{\frac{-2k}{k-1}}\right)d_X - \frac{8}{k}\frac{A_o V_o}{D_o U_o}\left(1 - \frac{1}{k-1}A_o^{\frac{-2k}{k-1}}\right)a$$

$$+ \frac{4V_o}{D_o^2}\left\{1 - \frac{A_o^2}{kU_o}\left(1 - A_o^{\frac{-2k}{k-1}}\right)\right\}d \qquad (I.31)$$

$$h = \frac{8A_o}{kD_o}\left(1 + \frac{1}{k-1}A_o^{\frac{-2k}{k-1}}\right)a - \frac{4A_o^2}{kD_o^2}\left(1 - A_o^{\frac{-2k}{k-1}}\right)d \qquad (I.32)$$

## APPENDIX J: REFERENCES

### Cited references


1. Edgerton, H.E. and Cathou, P.Y., "Xenon Flash Tube of Small Size". Rev. Sci. Instr., (10), 27, 821, (1956).

2. Hartmann, J., "On the Production of Acoustic Waves by means of an Air-jet of a Velocity exceeding that of Sound". Phil. Mag. (7) 11, 926 (1931). A number of related papers by the same author are cited.

3. Lettau, E., Deutsche Kraftfahrtforschung. 39, 1 (1939).

4. Frederiksen, E., "Resonance Behaviour of Non-Linear One-Dimensional Gas Vibrations Analyzed by the Ritz-Galerkin Method". Ing. Arch. 25, 100 (1957).

5. Betchov, R., "Nonlinear Oscillations of a Column of Gas". Phys. Fluids (3) 1, 205 (1958).

6. Sprenger, H., "Über thermische Effekte in Resonanzrohren". Mitteil. Inst. Aerodynamik, Zurich, Nr. 21 (1954).

7. Howick, P., and Hughes, R., "Pressure and Temperature Effects in Resonance Tubes". S.B. thesis, M.I.T., (1958).

8. Cassidy, E., Thompson, R., and Slawsky, M., unpublished research at the National Bureau of Standards, (1957).

9. Sibulkin, M., and Vrebalovich, T., "Some Experiments with a Resonance Tube in a Supersonic Wind Tunnel". Readers Forum, Jour. Aero-Space Sc. (7) 25, 465 (1958).

10. Lloyd, E., unpublished research at the National Bureau of Standards, (1958).

11. Fam, S., "A Photographic Study of Resonance Tubes". S.M. thesis, M.I.T., (1960).

12. Hartenbaum, B., "Hydraulic Analogue Investigation of the Resonance Tube". S.M. thesis, M.I.T., (1960).

13. Sprenger, H., "Neue Erkenntnisse über thermische Effekte beim Expandieren von Gasen". Zeit. Schweisstechnik 10, 3 (1956).

14. Emden, R., "Über Ausstromungserscheinigungen Permanenter Gase". Habilitationsschrift, Leipzig, (1899). Extracts from this dissertation appear in Wied. Ann. Physik. 69, 264 and 426 (1899).

15. Prandtl, L., "Über die stationären Wellen in einem Gasstrahl". Physik. Zeit. 19, 5, 599 (1904).

16. Hartmann, J., and Lazarus, F., "The Air-Jet with a Velocity exceeding that of Sound". Phil. Mag. (7), 31, 35 (1941).

17. Merle, M., "Sur la structure d'un jet d'air a grande vitesse". Compt. Rend. 240, 20, 1972 (1955).

18. Adamson, T., and Nicholls, J., "On the Structure of Jets from Highly Underexpanded Nozzles into Still Air." Jour. Aero-Space Sc. (1), 26, 16 (1959).

19. Shapiro, A.H., "On the Maximum Attainable Temperature in Resonance Tubes". Jour. Aero-Space Sc., Readers Forum, (1) 27, (1960).

20. Shapiro, A.H., "The Dynamics and Thermodynamics of Compressible Fluid Flow". Vol II, New York, Ronald Press, (1954).

21. Pai, Shih-I, "Fluid Dynamics of Jets". New York, D. Van Nostrand Co., (1954).

22. Mawardi, O., "On Acoustic Boundary Layer Heating". J. Acoust. Soc, Am. (5), 26, 726, (1954).

23. Sauer, R., "Introduction to Theoretical Gas Dynamics". Ann Arbor, J.W. Edwards, (1947).

Additional pertinent references


24. Ladenburg, R., Van Voorhis, Winkler, "Interferometric Studies of Faster than Sound Phenomena". Part II-Analysis of Supersonic Air-Jets . Phys. Rev. 76, 662 (1949).

25. Von Neumann, J., and Richtmyer, R., "A Method for the Numerical Calculation of Hydrodynamic Shocks". J. Appl. Phys., 21, 232 (1950).

    Shocks can be treated by a method involving the use of a viscosity-equivalent term in the numerical equations. The result is continuous property changes across the computed shocks in a flow. See also, Richtmyer's book.

26. Slezkin, N.A., "On the Impact of a Plane Gas Jet on an Infinite Wall". (in Russian), Prikl. Mat. Mekh. (2), 16, 227 (1952).

27. Elder, F.K., and deHaas, N., "Experimental Study of the Formation of a Vortex Ring at the Open End of Cylindrical Shock Tube". J. Appl. Phys. (10), 23, 1065 (1952).

28. Keller, J.B., "Finite Amplitude Sound Waves". J. Acoust. Soc. Am. (2), 25, 212 (1953).

    The standing wave in a closed tube and the progressive wave from a vibrating piston are considered.

29. Glass, I.I., et al, "A Theoretical and Experimental Study of the Shock Tube". Inst. of Aerophysics, Univ. of Toronto, UTIA Report No. 2 (1953).

    Section 5.08 contains Schlieren photographs of shock waves emerging from a shock tube into still air.

30. Mucklow, G., and Wilson, A., "The Attenuation and Reflection of Pressure Waves Propogated in Pipes". Parts I, II, Inst. Mech. Engrs. Proc., (1954).

31. Chisnell, R.F., "The Normal Motion of a Shock Wave through a Non-Uniform One-Dimensional Medium". Proc. Roy. Soc., London (A), 1190, 350, (1955).

32. Rudinger, G., "On the Reflection of Shock Waves from an Open End of a Duct". J. Appl. Phys. (8), 26, 1381, (1955).

The decay of pressure when a shock wave is incident on a duct end is treated acoustically.

33. Holt, M., "The Method of Characteristics for Steady Supersonic Rotational Flow in Three Dimensions". J. Fl. Mech., 1, 409, (1956).

34. Griffith, W.C., "Interaction of a Shock Wave with a Thermal Boundary Layer". J. Aero. Sc. (1), 23, 16, (1956).

Experimental and theoretical results for weak shocks with moderately heated (up to 80 °C) surfaces.

35. Boyer, D.W., "Effects of Kinematic Viscosity and Wave Speed on Shock Wave Attenuation". Inst. of Aerophysics, Univ. of Toronto, TN 8, (1956).

36. Hess, R.V., "Interaction of Moving Shocks and Hot Layers". NACA, TN, 4002, (1957).

37. Dosanjh, D.S., "Experiments on Interaction between a Traveling Shock Wave and a Turbulent Jet". J. Acoust. Soc. Am., (5), 26, 726, (1957).

38. Richtmyer, R.D., "Difference Methods for Initial Value Problems". New York, Interscience Publishers, Inc., (1957).

39. Bednarczyk, H., "The Stability of Normal Shocks". (in German), Ost. Ing. Z., (2), 1, 85, (1958).

40. Kontorovich, V.M., "Concerning the Stability of Shock Waves". translated from Russian by Am. Inst. Phys., JET P, (6), 6, 1179, (1958).

41. Oswatitsch, K., and Teipel, I., "Die Pulsationen von Stossdiffusoren". Zeit. Ang. Math. u Ph., (Zamp), IXb, 462, (1958).

42. Johnson, R.H., "Instability in Hypersonic Flow about Blunt Bodies". Phys. of Fluids (5), 2, 526, (1959).

A violent instability in the hypersonic flow of helium over blunt bodies with cavities is discussed.

## BIOGRAPHICAL NOTE

The author received his S.B. (1957) and S.M. (1958) degrees from Rensselaer. He was there a member of Pi Tau Sigma, Tau Beta Pi and Sigma Xi, and was awarded the Ricketts Prize in Mechanical Engineering.

His study at M.I.T. was under a National Science Foundation fellowship. He has been employed by the Albany Felt Co., Albany, New York and the Microtech Research Corp., Cambridge, Massachusetts.